Inhibitors and Antibody Fragments as Potential Anti-Inflammatory Therapeutics Targeting Neutrophil Proteinase 3 in Human Disease

Brice Korkmaz, Adam Lesner, Carla Guarino, Magdalena Wysocka, Christine Kellenberger, Hervé Watier, Ulrich Specks, Francis Gauthier, and Dieter E. Jenne

INSERM U-1100, Centre d'Etude des Pathologies Respiratoires and Université François Rabelais, Tours, France (B.K., C.G., F.G.); Faculty of Chemistry, University of Gdansk, Gdansk, Poland (A.L., M.W.); Architecture et Fonction des Macromolécules Biologiques, Unité Mixte de Recherche 7257, Marseille, France (C.K.); Génétique, Immunothérapie, Chimie et Cancer, Unité Mixte de Recherche 7292, Université François Rabelais, Tours, France (H.W.); Thoracic Diseases Research Unit, Division of Pulmonary and Critical Care Medicine, Mayo Clinic and Foundation, Rochester, Minnesota (U.S.); Comprehensive Pneumology Center, Institute of Lung Biology and Disease, German Center for Lung Research, Munich, Germany (D.E.J.); and Max Planck Institute of Neurobiology, Planegg-Martinsried, Germany (D.E.J.)

Abstract——Proteinase 3 (PR3) has received great scientific attention after its identification as the essential antigenic target of antineutrophil cytoplasm antibodies in Wegener's granulomatosis (now called granulomatosis with polyangiitis). Despite many structural and functional similarities between neutrophil

elastase (NE) and PR3 during biosynthesis, storage, and extracellular release, unique properties and pathobiological functions have emerged from detailed studies in recent years. The development of highly sensitive substrates and inhibitors of human PR3 and the creation of PR3-selective single knockout mice led to the identification of nonredundant roles of PR3 in cell death induction via procaspase-3 activation in cell cultures and in mouse models. According to a study in knockout mice, PR3 shortens the lifespan of infiltrating neutrophils in tissues and accelerates the clearance of aged neutrophils in mice. Membrane exposure of active human PR3 on apoptotic neutrophils reprograms the response of macrophages to phagocytosed neutrophils, triggers secretion of proinflammatory cytokines, and undermines immune silencing and tissue regeneration. PR3-induced disruption of the anti-inflammatory effect of efferocytosis may be relevant for not only granulomatosis with polyangiitis but also for other autoimmune diseases with high neutrophil turnover. Inhibition of membrane-bound PR3 by endogenous inhibitors such as the α-1-protease inhibitor is comparatively weaker than that of NE, suggesting that the adverse effects of unopposed PR3 activity resurface earlier than those of NE in individuals with α-1-protease inhibitor deficiency. Effective coverage of PR3 by anti-inflammatory tools and simultaneous inhibition of both PR3 and NE should be most promising in the future.

I. Introduction

Neutrophils, together with residential tissue macrophages, constitute the first very fast-reacting line of defense against pathogens. Neutrophils in particular produce and secrete large amounts of proteases, which contribute to the innate as well as the adaptive arms of host defense (Borregaard, 2010; Nauseef and Borregaard, 2014). Proteinase 3 (PR3), identified in 1978 and first called "myeloblastin," is an abundant serine protease of neutrophil granules (Baggiolini et al., 1978) (Table 1). Its mRNA is transcribed during the promyelocytic and promonocytic stages of myeloid differentiation (Bories et al., 1989; Zimmer et al., 1992; Monczak et al., 1997). It is stored mainly with other cathepsin (Cat) C–activated neutrophil serine proteases (NSPs) human neutrophil elastase (HNE), CatG, and NSP4 in the primary granules of circulating neutrophils. Exposure of neutrophils to cytokines and other chemoattractants leads to rapid granule translocation to the cell surface, with secretion of PR3 and other NSPs into the extracellular medium (Owen and Campbell, 1999). Purified quiescent human neutrophils from the peripheral blood of healthy individuals express a variable amount of PR3 on their surface (called constitutive PR3) (Csernok et al., 1990; Halbwachs-Mecarelli et al., 1995). Upon neutrophil activation, an additional amount of PR3 is exposed on the neutrophil cell surface (called induced PR3) (Korkmaz et al., 2009). PR3 exhibits structural and physicochemical properties similar to HNE (Hajjar et al., 2010).

The traditional view of PR3 and other NSPs being destructive scissors for degrading and eliminating microbes and tissues (Janoff and Scherer, 1968; Baggiolini et al., 1979; Kao et al., 1988) is complemented by new perspectives on their role in regulating cellular processes, innate immune responses, and tissue remodeling (Pham, 2006, 2008; Kessenbrock et al., 2011). Using genetically modified mice that lack one or a combination of these protease encoding genes, it is possible to analyze the molecular defects and alterations in neutrophil-mediated responses, in cell migration, and in clinical disease models after elimination of these proteases. The four NSPs (PR3, NE, CatG, and NSP4) are locally released together in response to pathogens and many other noninfectious danger signals. Under emergency conditions, they can accelerate immune responses and inflammation by inactivating anti-inflammatory mediators or by converting chemokine precursors into more bioactive isoforms.

The activities of NSPs are mainly controlled by the inhibitors belonging to the serpin family, such as α-1-protease inhibitor (α1PI) and α-1-antichymotrypsin, and the chelonianin family, such as elafin and secretory leukocyte protease inhibitor (SLPI) (Zani et al., 2009; Korkmaz et al., 2010; Scott et al., 2011; Wilkinson et al., 2011). In pathologic conditions, the balance between NSPs and inhibitors is disturbed and PR3 together with the other NSPs contributes to tissue damage, such as in chronic inflammatory lung diseases like chronic obstructive pulmonary disease (COPD), emphysema, and cystic fibrosis (Korkmaz et al., 2008b, 2010). NSPs are able to degrade many critical components of the extracellular matrix, including elastin, collagen, fibronectin, and laminins. It is important to note that endogenous inhibitors preferentially inhibit HNE when these neutrophil proteases are secreted by activated neutrophils (Korkmaz et al., 2013a). PR3 may thus play a more important role in tissue injury and as an accelerator of inflammation. Synergistic involvement of NSPs including PR3 in lung tissue damage was recently demonstrated in mice, with a triple deficiency of NSPs showing better protection against smoke-induced emphysema

TABLE 1
Relevant benchmarks in research on human PR3

Year	Benchmark	Reference
1978	Identification of PR3 as the third elastase-like protease	Baggiolini et al., 1978
1988	Elastolytic activity of PR3 showed in vivo	Kao et al., 1988
1989	Role of PR3 in cell differentiation attributed	Bories et al., 1989
1990	First synthetic inhibitors of PR3 reported	Groutas et al., 1990
	cDNA cloning of PR3 performed	Campanelli et al., 1990
	PR3 identified as the target antigen for C-ANCA	Jenne et al., 1990
	PR3 detected on the neutrophil cell surface	Csernok et al., 1990
1991	First biochemical and enzymatic characterization of PR3 performed	Rao et al., 1991
	Inhibition of PR3 by elafin investigated	Wiedow et al., 1991
1992	Gene mapping of PR3 performed	Sturrock et al., 1992
	Substrate binding site of PR3 mapped using synthetic substrates and inhibitors	Brubaker et al. Kam et al., 1992a,b
1993	PR3 gene (PRTN3) localized on 19p13.3	Sturrock et al., 1993
	Interaction of PR3 with SLPI investigated	Rao et al., 1993
1995	Bimodal distribution of PR3 on resting neutrophil surface observed	Halbwachs-Mecarelli et al., 1995
1996	Recombinant production of PR3 in human mast cell line-1 cells as active enzyme performed	Specks et al., 1996
	Crystal structure of PR3 identified	Fujinaga et al., 1996
1999	PR3 detected in secretory vesicles	Witko-Sarsat et al., 1999
	Mouse anti-PR3 mAbs were characterized and four separate epitopes areas on PR3 were identified	Van der Geld et al., 1999
2004	CatC identified as its endogenous activator	Pham et al., 2004
	Role of PR3 in cell apoptosis attributed	Pendergraft et al., 2004
	First selective FRET substrates of PR3 developed	Korkmaz et al., 2004
2005	PR3 is colocalized with $Fc\gamma RIIIB$ in neutrophil lipid raft	David et al., 2005
2007	NB1 (CD177) is identified as a PR3[m] receptor	von Vietinghoff et al., 2007
2008	Unique hydrophobic cluster of PR3 identified as its membrane binding area	Korkmaz et al., 2008a
2009	Enzymatic characterization of PR3[m] performed	Korkmaz et al., 2009
	PR3 is identified on neutrophil extracellular traps	Kessenbrock et al., 2011
2010	Conformational epitopes of PR3 mapped	Kuhl et al., 2010 Silva et al., 2010
2011	First recombinant selective protein inhibitor of PR3 developed: serpinB1(STDA/R)	Jégot et al., 2011
2012	First cell-permeable FRET substrate of PR3 synthesized	Wysocka et al., 2012
	First synthetic substrate-like inhibitor of PR3 developed: azapro-3	Epinette et al., 2012
2013	First mAb completely altering activity of PR3 identified: MCPR3-7	Hinkofer et al., 2013
2014	First PR3 activity-based probe developed	Guarino et al., 2014
	Altered conformation and activity of PR3[m] reported	
2015	Allosteric modulation of PR3 activity by C-ANCA reported	Hinkofer et al., 2015
	Endothelial cytoskeletal target substrates of PR3 identified	Jerke et al., 2015

than single elastase-deficient knockout mice (Guyot et al., 2014). Apart from causing tissue injury, PR3 and other NSPs stimulate the release of cytokines and enhance their bioactivities, thereby triggering excessive inflammatory responses (Kessenbrock et al., 2011).

PR3 stands out against the other three NSPs because it is the primary antigenic target of autoantibodies, such as antineutrophil cytoplasmic autoantibodies (ANCAs) in granulomatosis with polyangiitis (GPA; formerly known as Wegener's granulomatosis) (Jenne et al., 1990). GPA, a relatively uncommon chronic inflammatory disorder, is characterized by necrotizing granulomatous inflammation and vasculitis of small blood vessels (Jennette et al., 2011; Tadema et al., 2011). The interaction of pathogenic ANCAs with membrane-bound proteinase 3 (PR3[m]) results in an excessive activation of neutrophils with production of reactive oxygen species and release of various granule-stored proteases into the pericellular environment (Hu et al., 2009; Kettritz, 2012). Tumor necrosis factor-α–primed neutrophils are less sensitive to activation by anti-PR3 monoclonal antibodies (mAbs) after they have been incubated with an excess of α1PI, the major endogenous inhibitor of PR3 found in plasma (Guarino et al., unpublished data). This suggests that the binding of α1PI to neutrophil membranes, and the removal of active PR3[m] from the cell surface, decreases mAb binding and proinflammatory signaling (Rooney et al., 2001; Korkmaz et al., 2009; Jégot et al., 2011). ANCA pathogenicity and neutrophil activation may therefore depend on the (local) levels and inhibitory activity of α1PI. This role of α1PI in GPA is supported by the observation that α1PI deficiency is a genetic risk factor for ANCA-associated vasculitis (Lyons et al., 2012). As α1PI complexes with HNE at a faster rate, PR3 remains uninhibited for a longer period of time and diffuses further into tissues

than HNE (Korkmaz et al., 2005a, 2013a; Sinden et al., 2015). Moreover, PR3^m was shown to inhibit the phagocytosis of apoptotic neutrophils by binding to calreticulin on apoptotic neutrophils (Gabillet et al., 2012). During neutrophil aging and conditions of lysosomal membrane rupture, granule-associated PR3 reaches the cytosol and activates procaspase-3 (Loison et al., 2014). In this way, PR3 can accelerate neutrophil cell death and the removal of neutrophils from inflamed tissues. However, the proapoptotic activity of PR3 in the cytosol is counterbalanced by serpinB1, which declines in aged neutrophils (Loison et al., 2014).

Recent data demonstrate that ANCA-induced PR3 release triggers specific cellular responses in endothelial cells during vascular inflammation. Secreted PR3 can be recaptured and internalized by endothelial cells, which coincides with the activation of proapoptotic signaling events through extracellular signal-regulated kinase, c-Jun N-terminal kinase, and p38 mitogen-activated protein kinase (Preston et al., 2002). Upon its entry, PR3 can usurp the cell's control of its own fate by directly interfering with caspase cascades. Crosstalk between neutrophils and endothelial cells at sites of inflammation affects both cytokine networks and cell viability. Jerke et al. (2015) recently identified 82 novel endothelial proteins cleaved by PR3 and other NSPs and generated extended cleavage signatures for NSPs (Table 1). Most of the identified proteins are cytoskeletal proteins, and inhibition of NSPs activity in vitro preserved the endothelial cytoskeletal structure. Active PR3 as well as other NSPs thus appear to be a therapeutic target for active site–directed selective inhibitors to protect small blood vessels from neutrophil-induced cell death.

A large number of studies have provided significant evidence that PR3 contributes to inflammatory tissue damage at different levels (Box 1) and can be regarded as a promising therapeutic target (Korkmaz et al., 2010, 2013b; Jerke et al., 2015). In this review, we first provide an overview of PR3, its functional biochemistry, and protein/chemical inhibitors. We then focus on anti-PR3 antibodies that can alter PR3 activity and mask ANCA epitopes. Finally, we discuss the potential application of inhibitors and antibody fragments as anti-inflammatory agents to mitigate the pathogenic effects of PR3 in human disease.

II. Structure, Biosynthesis, and Physicochemical Properties of Proteinase 3

PR3 belongs to the family of chymotrypsin/trypsin-fold serine proteases having evolved from a common ancestor. Serine proteases are proteolytic enzymes that catalyze the hydrolysis of peptide bonds by a serine-directed nucleophilic attack mechanism, which ultimately results in irreversible processing of the target peptides or proteins (Hedstrom, 2002). The chymotrypsin/trypsin-fold proteases use a catalytic triad for proteolytic activity composed of the highly conserved His57, Asp102, and Ser195 residues (chymotrypsinogen numbering), which are located at the junction of the two β-barrels. By contrast, the active site cleft runs perpendicular to this junction. This arrangement of amino acids in the active site presumably allows nucleophilic attack by Ser195 on the carbonyl carbon (C = O) of the substrate scissile bond, thus setting off the catalysis process. Several residues localized on the loops surrounding the active site assist the catalysis. The oxyanion hole defined by the backbone amide hydrogens of Ser195 and Gly193 and located near the carbonyl group of the substrate's scissile bond (Fig. 1) stabilizes the developing partial charge on the tetrahedral intermediate during catalysis (Hedstrom, 2002).

All chymotrypsin/trypsin-fold proteases are synthetized as inactive zymogen precursors that are irreversibly processed (Jenne and Kuhl, 2006). Several crystal structures of serine proteases such as trypsin or chymotrypsin have been published alone or in complex with various inhibitors. Several crystal structures for HNE have been deposited in the Protein Brookhaven Database. By contrast, only one crystallographic study for human PR3, which used recombinant PR3 from Chiron Technologies, has been published (Fujinaga et al., 1996). The scarcity of structural data appears to be directly linked to the difficulties of purifying natural PR3 and producing recombinant soluble PR3, mainly because of its hydrophobic character. Like other members of this family, PR3 consists of two homologous β-barrels and a C-terminal helix (Fujinaga et al., 1996) (Fig. 1). Each barrel contains six antiparallel β-sheets connected through a linker segment. The PR3 polypeptide chain is stabilized by four disulfide bridges.

Chymotrypsin/trypsin-fold proteases have similar tertiary structures but differ in their substrate specificity, which is governed by their substrate binding pockets. The S1 pocket of these proteases plays a major role in defining the new C terminus of the cleaved fragment and accommodates the side chain of the residue preceding the scissile bond. The S1 pocket is formed by residues 189–195, 214–220, and 225–228.

BOX 1 Pathogenic roles of PR3
1) Secreted PR3
    Participates in tissue degradation
    Promotes inflammation
2) Cytosolic PR3
    Enhances apoptosis in neutrophils
    Induces apoptosis in endothelial cells
3) Membrane-bound PR3
    Enhances ANCA-induced proinflammatory
      response of primed neutrophils
    Enhances proinflammatory response of
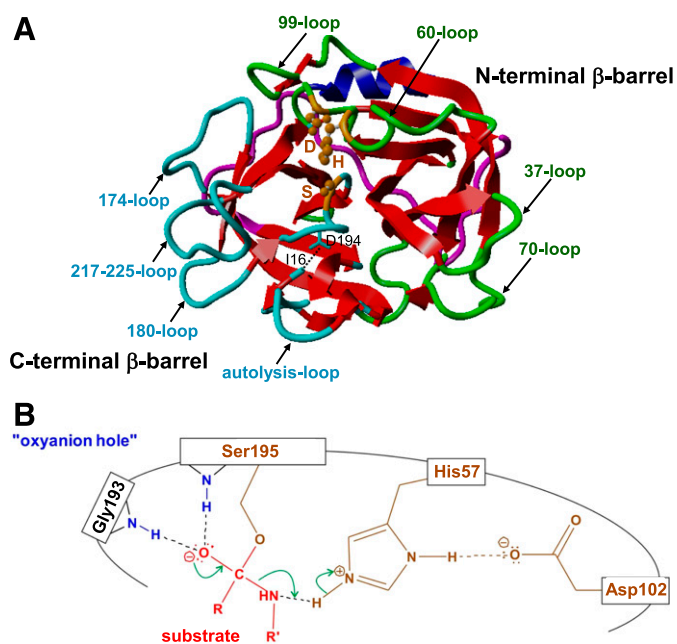   apoptotic neutrophils

A

B

Fig. 1. Three-dimensional structure of PR3 and its catalytic triad (charge-relay system). (A) The ribbon plot based on the atomic coordinates of PR3 (Protein Data Bank code 1FUJ; Fujinaga et al., 1996) showing two asymmetric β-barrels and C-terminal α-helix. The flexible loops of the N-terminal and C-terminal β-barrels are depicted in green and in cyan, respectively. The catalytic triad [His57, Asp102, and Ser195 (chymotrypsin numbering)] are shown in a ball-and-stick representation. The catalytic triad residues are indicated by their single-letter codes in brown. The representation was generated with Yasara (http://www.yasara.org). (B) The catalytic triad (charge relay system) of chymotrypsin/trypsin-fold serine proteases. The oxyanion of the backbone amide hydrogens of Ser195 and Gly193 stabilizes the charge build-up on the substrate transition state.

The three major classes of side chain specificities at the P1 position are determined by the structural features of the S1 pocket and are classified as trypsin like, chymotrypsin like, and elastase like. Trypsin-like proteases display a deep open acidic S1 pocket and accept the side chain of an arginine or a lysine residue. Substrate recognition is mediated by a salt bridge with the highly conserved Asp189 at the bottom of the S1 pocket. Chymotrypsin-like proteases have an open hydrophobic pocket and preferentially accommodate bulky P1 residues. Elastase-like proteases have a shallow hydrophobic S1 pocket formed by the residues at positions 190 and 216 and only cleave after small hydrophobic residues. PR3 displays an elastase-like S1 pocket with a partially occluded S1 pocket and cleaves after small hydrophobic residues (Fig. 2). The recently discovered fourth NSP, NSP4, with trypsin-like specificity has a fully occluded S1 pocket (Lin et al., 2014).

The gene encoding PR3 (*PRTN3*) consists of five exons and four introns and is located in the terminal region of the short arm of chromosome 19p13.3 (Sturrock et al., 1992, 1993; Zimmer et al., 1992). PR3 mRNA is detected in early progenitor cells of the myeloid and monocytic lineage. It is transcribed only in the promyelocyte stages of myeloid differentiation (Wong et al., 1999). Upon granulocyte differentiation, transcription of PR3 mRNA

is downregulated (Zimmer et al., 1992; Sturrock et al., 1996). PR3 is expressed as an inactive pre-proprotein containing a signal peptide, an amino-terminal prodipeptide, and a C-terminal propeptide. After the 25 residues of the signal peptide are removed, the nascent polypeptide chain of the PR3 molecule starts with the amino-terminal prodipeptide sequence Ala-Glu, which maintains the pro-PR3 in its zymogen conformation with a disordered active site. The subsequent processing of the N-terminal dipeptide by CatC (a conserved tetrameric cysteine protease, also called dipeptidyl peptidase I; Turk et al., 2001) leads to mature PR3 (Adkison et al., 2002). This processing allows insertion of the amino terminus into the interior of the molecule, where the free NH^{3+} group of the first N-terminal residue Ile16 forms a salt bridge with the Asp194 next to the active site Ser195 (Fig. 1A). This interaction results in a reorientation and remodeling of three flexible surface loops (the 217–225 loop, the 180 loop, and the so-called autolysis loop) and their respective side chains within the so-called activation domain (Pozzi et al., 2012). This conformational modification renders the active-site S1 pocket (nomenclature of Schechter and Berger, 1967) of the PR3 accessible to substrates and inhibitors. The removal of the C-terminal propeptide containing eight residues (Arg-Val-Glu-Ala-Lys-Gly-Arg-Pro) does not affect proteolytic activity. In neutrophils, PR3 is identified as a triplet of isoforms of approximately 29–32 kDa, which differ by their carbohydrate structures at Asn102 and Asn147 (Zoega et al., 2012).

The proteolytically active mature PR3 without N-terminal and C-terminal propeptides is mainly stored in the azurophilic granules of neutrophils (Campanelli et al., 1990), but it is also found on the outer membrane and in the lumen of secondary granules and secretory vesicles (Witko-Sarsat et al., 1999). Variable amounts of PR3 are also constitutively expressed on the cellular surface of quiescent human neutrophils from the peripheral blood of healthy individuals (Csernok et al., 1990; Halbwachs-Mecarelli et al., 1995). Freshly purified neutrophils can be generally divided into two subsets that express low and high amounts of PR3 (Kettritz, 2008). NB1 or CD177, a glycosylphosphatidylinositol-anchored membrane protein, has been identified as a potential receptor of PR3 on the neutrophil cell surface (von Vietinghoff et al., 2007; Korkmaz et al., 2008a). The main characteristics of PR3 are listed in Table 2.

III. Structural Basis of Specific Proteinase 3 Functions

A. Recombinant Production

The biologic and pathophysiologic functions of PR3 are defined by its conformation and by its structural determinants (Specks, 2000). High amounts of purified PR3 are required to investigate its functions in
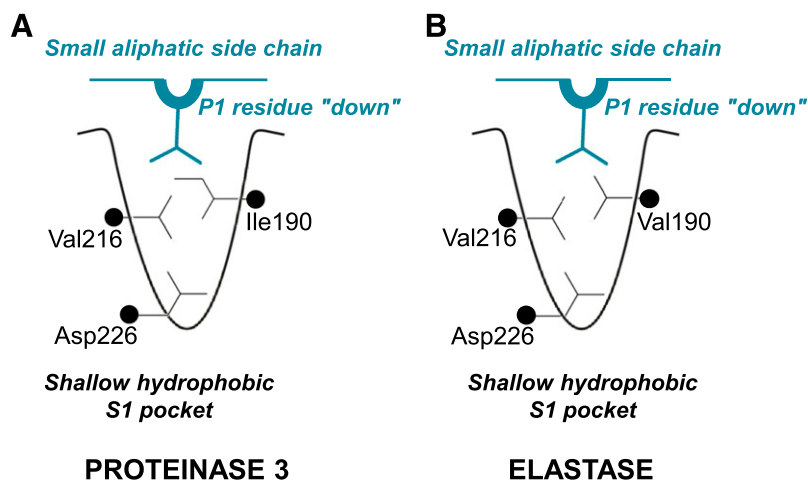
Fig. 2. Schematic model of S1 pockets from PR3 and elastase. (A) The S1 pockets of PR3 and elastase are shallow and hydrophobic. (B) Ile190/Val216 on PR3 and Val190/Val216 on elastase confine their S1 pockets to small alkyl side chains (Fujinaga et al., 1996).

vitro. Purification of the native catalytically active PR3 from granulocytes is relatively inefficient, time-consuming, and technically demanding. During the purification procedure, conformational changes, partial aggregation, and denaturation and adsorption on surfaces reduce the final yield of PR3. Recombinant production of PR3 is an alternative to obtain high amounts of functional proteinase. Moreover, recombinant variants of PR3 offer many advantages over the natural antigen, such as the identification of the structural determinants of the proteins (e.g., epitope mapping).

The cDNA of PR3 has been expressed in prokaryotic and eukaryotic cell systems. Refolding of bacterially produced inclusion bodies was unsuccessful. Correct conformational identity, post-translational modifications, and antigen stability can be achieved by the expression of PR3 in insect or mammalian cells. Expression of recombinant PR3 in insect cells was disappointing because the recombinant PR3 product did not have a well enough preserved conformation to serve as a target antigen for ANCA recognition in diagnostic assays. Moreover, the Sf9 insect cells resulted in aberrant glycosylation of PR3 (Fujinaga et al., 1996; Witko-Sarsat et al., 1996; van der Geld et al., 2000). Hematopoietic cell lines such as human mast cell line-1 or rat basophilic leukemia-1 cells produce active serine proteinases in storage granules and are more similar to human neutrophils (Specks et al., 1996, 1997; Garwicz et al., 1997). However, the purification of recombinant PR3 from subcellular organelles was laborious and inefficient in a previous study (Jenne et al., 1997). Alternatively, nonhematopoietic cell lines, such as human embryonic kidney 293 (HEK293) cells and Chinese hamster ovary cells lacking a regulated pathway of protein secretion, can be used for the recombinant expression of PR3 because they constitutively secrete the unprocessed PR3 zymogen into the cell culture supernatant after transfection (Sun et al.,

1998; Korkmaz et al., 2008a). These cells constitutively secrete significant amounts of the N- and C-terminally unprocessed PR3 zymogen into the cellular medium, allowing for both N- and C-terminal customized modifications (Sun et al., 1998; Capizzi et al., 2003). PR3 with the conformation of the mature enzyme can be expressed in such mammalian expression systems by transfecting cDNA plasmids that code for a PR3 variant lacking the two–amino acid propeptide (Sun et al., 1998). However, to prevent cell death resulting from premature intracellular activation of the recombinant PR3 after cleavage of the signal peptide, such recombinant PR3 versions also must carry the S195A substitution, which renders the PR3 enzymatically inactive without resulting in a significant change of its conformation (Specks et al., 1996; Sun et al., 1998). The C-terminal extension of six or seven residues of PR3 is reported to not be important for activity, intracellular sorting, and interactions with substrates/inhibitors or cytoplasmic antineutrophil cytoplasmic antibodies (C-ANCAs) (Capizzi et al., 2003). Subsequent purification and immobilization of recombinant PR3 is further simplified by the attachment of six histidine residues (a convenient tag) at the C-terminal end (Capizzi et al., 2003). In contrast with conventional capture techniques with murine mAbs, histidine tag-based immobilization of recombinant PR3 does not mask portions of the PR3 surface and facilitates antigen coating and antibody interactions with the immobilized antigen (Kuhl et al., 2010).

A different approach is preferable for the generation of enzymatically active recombinant PR3. Nearly pure six-His–tagged PR3 zymogen is obtained from serum-free culture media by nickel–nitrilotriacetic acid chromatography in a single step (Korkmaz et al., 2008b; Kuhl et al., 2010). After purification, the amino-terminal peptide has to be cleaved precisely to obtain the proper three-dimensional conformation and activity. The in vitro conversion of the Ala-Glu-PR3 zymogen

TABLE 2
Main characteristics of human PR3

Characteristic	Description
EC number	EC 3.4.21.76
Crystal structure	Protein Data Bank accession code 1FUJ
Gene locus and gene structure	19p13.3, 5 exons, 4 introns
Propeptides	N-terminal prodipeptide: AE
	C-terminal propeptide: RVEAKGRP
Endogenous activator	CatC
	Removal of the N-terminal prodipeptide
Characteristics of mature forms	222 residues
	Molecular mass: 29–32 kDa
	pI: approximately 9.5
	Number of glycosylation sites: 2
	Number of disulfide bridges: 4
Polymorphisms	V/I92; A/T108; T/S109
Optimal pH for activity	Approximately 8.0
Substrate specificity	Small hydrophobic residue at P1 position:
	(V, A, C, T, M)
Best FRET substrates	ABZ-VADnorVADYQ-EDDnp
	ABZ-YYAbuNEPY(NO$_2$)
	O$_2$Oc-K(HMC)-YYAbu-Orn(CM3) (cell-permeable)
Source	Neutrophil
	Monocyte
	Basophile
Localization in neutrophil	Azurophilic granules
	Specific granules
	Secretory vesicles
	On resting and activated neutrophil cell surface
	On neutrophil extracellular traps
Membrane-bound forms	Constitutive PR3 (on resting neutrophils)/inactive
	Induced PR3 (on activated neutrophils)/in activable conformation
Endogenous inhibitor	α2-macroglobulin
	α1PI/serpinB1
	Elafin/pre-elafin
Selective inhibitors	SerpinB1(STDA/R)
	Anti-PR3 mAb MCPR3-7
	ABZ-VAD(aza)norVADYQ-Y(NO$_2$) (azapro-3)
	ABZ-VADnV[Ψ](COCH$_2$)-ADYQ-EDDnp (keto-D-DY$_{FRET}$)
	HX-PYDA^P(-O-C$_6$H$_4$-4-Cl)$_2$
	Bt-[PEG]$_{66}$-PYDA^P(-O-C$_6$H$_4$-4-Cl)$_2$ (activity-based probe)
Biological functions	Degradation of extracellular matrix components
	Bactericidal properties
	Cleavage of inflammatory mediators
	Cleavage of receptors
Pathologic roles in human diseases	Chronic inflammatory diseases
	GPA
	Papillon–Lefèvre syndrome

AE, Ala-Glu; AHX, amino hexanoic acid; HX, hexanoic acid.

purified from the cell supernatant into catalytically active PR3 by CatC is expensive and relatively inefficient. The most reliable and currently preferred procedure is the PR3 production with a specifically engineered N-terminal extension containing a thrombin or an enterokinase cleavable prosequence (Korkmaz et al., 2008b; Kuhl et al., 2010). The DDDDK modification permits the removal of the N-terminal prosequence by endoproteolytic processing using bovine, porcine, or recombinant enterokinase. Subsequent in vitro processing removes this N-terminal extension and creates the natural mature PR3 N-terminus starting with Ile16. The extent of conversion is easily checked on SDS-PAGE by observing the reduction in molecular size, whereas complete removal of the natural sorting dipeptide by CatC is difficult to achieve and to control (Jenne and Kuhl, 2006; Kuhl et al., 2010).

B. Substrate Binding Sites

The crystal structure of uncomplexed recombinant PR3 (1FUJ) produced in insect cells was identified by molecular replacement using the structure of crystallized HNE (Fujinaga et al., 1996). Several three-dimensional structures of HNE complexed with the third domain of turkey ovomucoid (Bode et al., 1986), domain 2 of SLPI (Koizumi et al., 2008), and synthetic inhibitors have all been determined (Wei et al., 1988; Navia et al., 1989; Huang et al., 2008; Hansen et al., 2011; Lechtenberg et al., 2015). PR3 and HNE share a high sequence identity (56%) and display a common fold. However, substitutions in their S1 pockets and in the surface loops defining the environment of the active site (99 loop, 60 loop, 37 loop, and autolysis loop) give them distinct proteolytic cleavage specificities (Fujinaga et al., 1996; Korkmaz et al., 2007). On the

basis of their crystal structures, PR3 substrate binding sites are much more polar than those of HNE. Solvent-accessible surfaces in PR3 and HNE show that their charge distributions in the vicinity of the substrate binding region differ significantly (Korkmaz et al., 2007). PR3 displays four charged residues (Arg60, Asp61, Lys99, and Arg143) in the vicinity of the substrate binding cleft that extends from subsite S4 to subsite S3′ (Fujinaga et al., 1996; Korkmaz et al., 2007) (Fig. 3).

The S1 binding pocket of PR3 is hemispherical, but it seems to be smaller than that of HNE because of the Val/Ile substitution at position 190 (Fujinaga et al., 1996). The specificity of PR3 and HNE has been investigated using chromogenic substrates, such as p-nitroanilide (pNA), 5-Amino-2-nitrobenzoic acid, and thiobenzylester, and fluorogenic substrates, such as aminomethylcoumarin and fluorescence resonance energy transfer (FRET) substrates. Both PR3 and HNE preferentially accommodate small hydrophobic residues (Val, Cys, Ala, Met, Ile, and Thr) in the S1 pocket. Because of the Val/Ile substitution in the S1 subsite, PR3 cleaves proteins or peptides containing an Ala at the P1 position more efficiently than does HNE (Jégot et al., 2011).

The S2 subsite of PR3 is a deep polar pocket of increased polarity due to the presence of two positively solvent-accessible charged residues Arg and Lys at positions 60 and 99, respectively (Fujinaga et al., 1996). By contrast, the Lys/Leu substitution at position 99 makes the S2 subsite of HNE quite hydrophobic. PR3 preferentially accommodates a negatively charged (Asp, Glu) or a hydrophilic residue (Tyr, Ser) at P2 because of its Lys99 (Hajjar et al., 2006; Korkmaz et al., 2007, 2013a). The replacement of Lys99 by Leu in a recently described recombinant PR3 mutant (PR3K99L) considerably reduced the rate at which PR3 substrates were hydrolyzed (Jégot et al., 2011). These data suggest that Lys99 is a key residue involved in the proteolytic specificity of human PR3. By contrast, HNE preferentially cleaves sequences containing a hydrophobic residue at position P2. The residue at position 99 in PR3 and HNE borders both the S2 and S4 subsites, which makes them smaller and more polar in PR3 than in HNE. In addition, there is a charged arginyl residue at position 217 in HNE in the vicinity of S4, whereas it is an Ile in PR3. Our recent study using single-residue mutant PR3 with Arg at position 217 (PR3I217R) revealed that Ile217 in the vicinity of the S4 pocket greatly influences the substrate specificity of PR3 (Guarino et al., 2014).

PR3 and HNE also differ in their P3 specificity; only HNE preferentially accommodates a negatively charged residue at that position (Jégot et al., 2011). Most FRET substrates or peptides selectively cleaved by HNE have a negatively charged residue at position P3. Therefore, a PR3 substrate with a negatively charged residue at position P2 may be cleaved one bond downstream by HNE, which can accommodate this residue within its S3 subsite.

Molecular dynamics simulations based on the three-dimensional structure reveal that Asp61 in PR3 is close to the putative subsites S1′ and S3′, and Arg143 contributes to the shape of the S2′ pocket (Hajjar et al., 2006; Korkmaz et al., 2007). The 60 loop containing Asp61 is significantly displaced to bring the negatively charged side chain close to the S1′ and S3′ sites. The S1′ and S2′ subsites in HNE are relatively hydrophobic; S1′ is lined with Cys42–Cys58 and S2′ with Phe41 and Leu143. Peptidyl sequence elongation beyond P1′ has a favorable effect on PR3 hydrolysis but not on HNE hydrolysis. In addition, the charged residues Lys99, Arg143, and Asp61 confer specific biologic functions to PR3, which have been deduced from the identifications of specific cleavage sites within target proteins such as nuclear factor-κB, p21, pro–interleukin-8, and calmodulin (Fig. 3).

The widely used peptidyl-thiobenzylester and pNA substrates do not distinguish PR3 and HNE activities. We recently developed a selective biotinylated pNA substrate, Bt-Pro-Tyr-Asp-Ala-pNA (k_{cat}/K_m = approximately 30 mM^{-1}s^{-1}), for PR3 over HNE (Guarino et al., unpublished data). Structural differences between PR3 and HNE at S3, S2, S1′, and S2′ have been exploited to develop highly sensitive and specific synthetic FRET peptide substrates for human PR3 that allow its detection in complex biologic samples (Hajjar et al., 2006; Korkmaz et al., 2007; Popow-Stellmaszyk et al., 2013; Sinden and Stockley, 2013; Hinkofer et al., 2015). In addition, a cell-permeable selective PR3 substrate, O$_2$Oc-K(HMC)-YYAbu-Orn(CM3), was recently developed (Wysocka et al., 2012).

C. Antigenic Sites

C-ANCAs recognize conformational epitopes on the solvent-accessible surface of PR3 (9800 Å). Although PR3 and HNE share a very similar three-dimensional structure, C-ANCAs from patients with GPA do not crossreact with HNE. Mouse anti-PR3 mAbs generated by several investigators were reported to recognize different conformational epitopes on the PR3 surface and to interfere with the binding of PR3–C-ANCA. Biosensor technology, a flow cytometry assay based on TALON beads, and the capture enzyme-linked immunosorbent assay were used for epitope-specific grouping of mouse anti-PR3 mAbs (Van der Geld et al., 1999; Kuhl et al., 2010; Silva et al., 2010). A collection of 14 mouse anti-PR3 mAbs was characterized and grouped into four major subsets that recognize different surface regions of PR3 (Silva et al., 2010) (Fig. 4). Antigen surfaces that interact with conformational antibodies are on average 700–1000 Å in size (Sundberg and Mariuzza, 2002) and are expected to cover several amino acid residues on different surface loops.
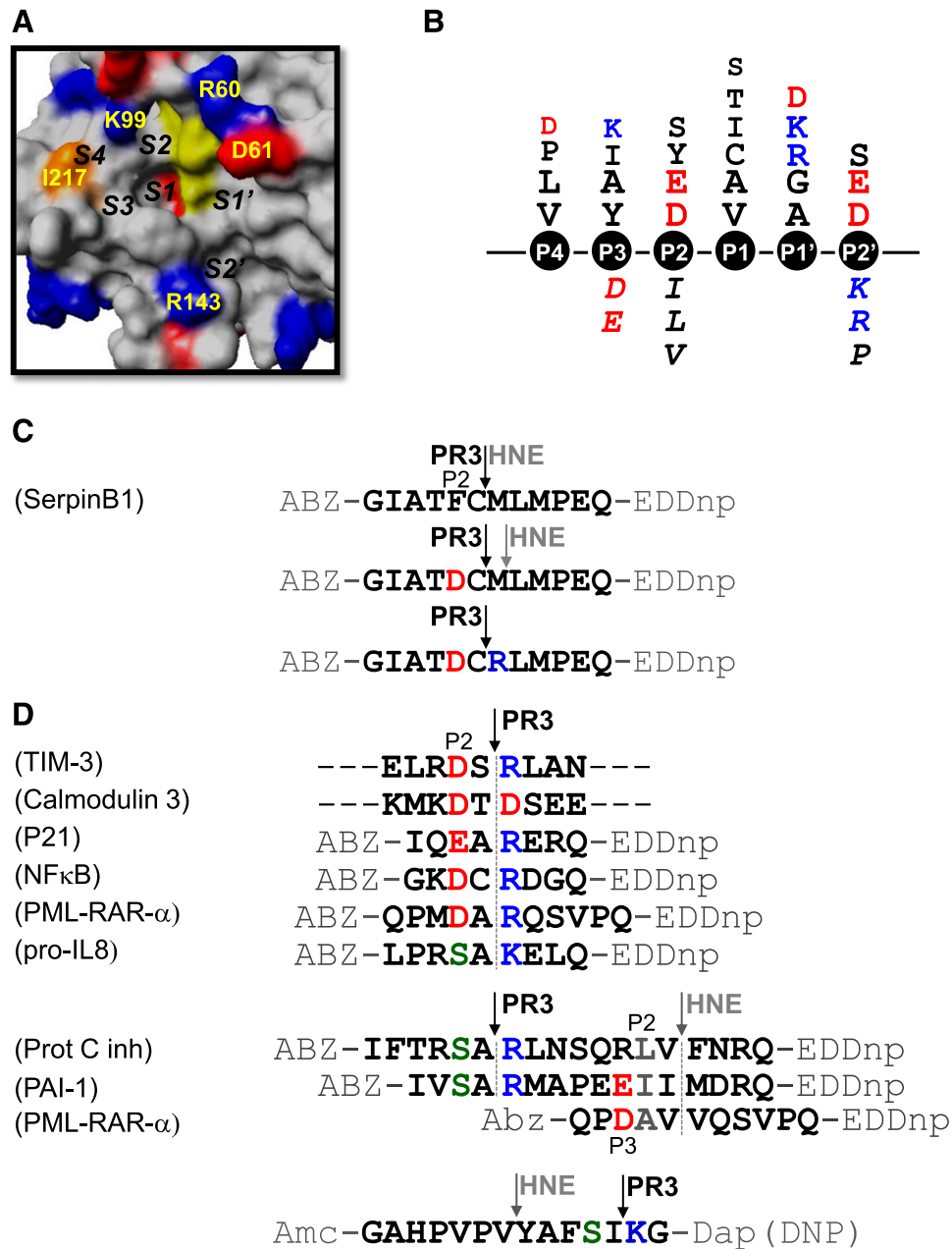
Fig. 3. Proteolytic profile and substrate specificity of PR3. (A) The solvent-accessible surface of substrate binding sites in PR3 (Protein Data Bank 1FUJ). The residues of the catalytic triad are in yellow. The single-letter code of critical charged residues in the vicinity of the active site is indicated in yellow. The position of the S and S′ subsites are indicated by black letters. (B) Subsite preference of PR3 for chromogenic and fluorogenic peptide substrates. The circles illustrate residues from P4 to P2′. The size of the single-letter codes for the different residues above the circles reflects the frequency of occurrence of residues at the P4 to P2′ positions. The residues below the circles are not well accommodated. (C) Conversion of a polyvalent FRET substrate to a selective substrate of PR3. Cleavage sites of PR3 and elastase in ABZ-peptidyl-EDDnp FRET substrates derived from the RCL of serpinB1 are indicated by arrows. PR3 accommodates a negatively charges residue at P2 position (shown in red), whereas elastase accommodates this residue at the P3 position and cleaves the substrate one bond further down from the cleavage site of PR3 (C-M). Substitution of the methionine by an arginine abolishes the cleavage of elastase. (D) Sequences in TIM-3 (Vega-Carrascal et al., 2011) and calmodulin 3 (Jerke et al., 2015) and FRET substrates derived from P21 (Korkmaz et al., 2007), NFκB, PML-RAR-α, pro-IL8 (Korkmaz et al., 2013a), protein C inhibitor (Korkmaz et al., 2013a), and PAI-1 (Korkmaz et al., 2002) that are selectively cleaved by PR3 and elastase. IL, interleukin; NFκB, nuclear factor κB; PAI-1, plasminogen activator inhibitor; PML-RAR-α, promyelocytic leukemia–retinoic acid receptor-α; TIM-3, T-cell Ig mucin domain-containing molecule 3.

Several attempts were made to identify structural determinants of PR3 antigenic sites. Natural PR3 homologs from granulocytes of mice and various primates permitted us to assess the extent of crossreactivity with human PR3 and the tentative location of conformational epitopes in view of the observed sequence variations in different mammalian species. Chimeric molecules composed of human PR3 and HNE or human/gibbon PR3 were also used for epitope mapping strategies (Selga et al., 2004; Kuhl et al., 2010). The natural substitutions found in the gibbon PR3 homolog, which are not equally distributed but are clustered on one side of the surface, allowed us to identify the conformational epitopes of the group 1 and group
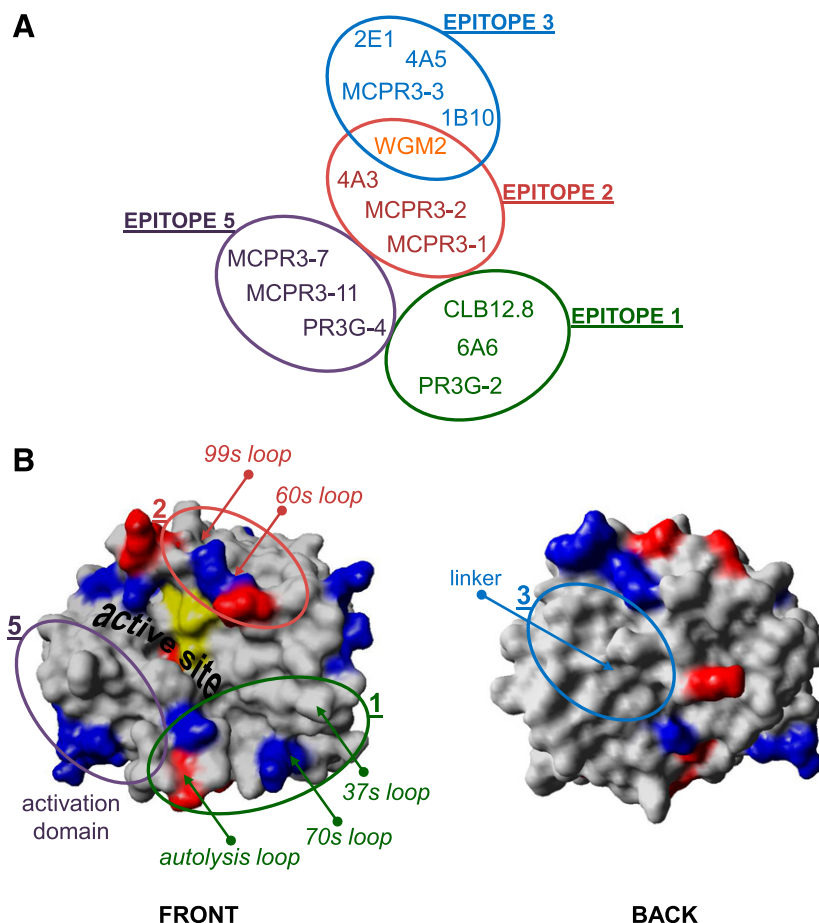
Fig. 4. Nonoverlapping epitopes recognized by four groups of murine mAbs on PR3. (A) Diagram showing the grouping of murine anti-PR3 mAbs (Kuhl et al., 2010; Silva et al., 2010). (B) Binding regions of different anti-PR3 mAbs. Solvent-accessible molecular surfaces with positive or negative electrostatic potential of PR3 are colored dark blue and red, respectively. The serine of the catalytic triad is yellow. Arabic numbers designate the four major surface epitopes recognized by the anti-PR3 mAbs (Kuhl et al., 2010; Silva et al., 2010). Epitope numbering corresponds to mAb grouping. The loops and the linker are indicated by the arrows. The representation was generated with Yasara.

4 mouse mAbs. Group 1 mAbs (CLB12.8, 6A6, and PR3G-2) bind to a region on PR3 formed mainly by two closely spaced surface loops: the 37 loop and the 70 loop (Fig. 4). In contrast with the other identified epitopes, epitope 1 is altered by α1PI binding that induces a conformational change. Group 2 mAbs (MCPR3-1, MCPR3-2, and 4A3) bind to a region of the N-terminal subdomain located north of the substrate binding cleft composed by the 60 loop and the beginning of the long 99 loop. Group 3 mAbs (4A5, WGM2, 1B10, 2E1, and MCPR3-3) recognize an antigenic region located on the back of PR3 (Fig. 4). This region contains a segment that connects the N- and C-terminal β-barrels. Minor sequence modifications on this segment between positions 119 and 122 led to a loss of the binding site (Kuhl et al., 2010; Silva et al., 2010). Novel mAbs named MCPR3-7 and MCPR3-11 that map to epitope 5 are unique because they bind much better to proPR3 than to mature PR3.

A vast majority of C-ANCAs share binding specificity with group 1 mAbs (CLB12.8, 6A6, and PR3G-2) because they cannot bind to PR3 in complex with α1PI (Kuhl et al., 2010). In addition, several studies reported that purified C-ANCAs were able to interfere with the proteolytic activity of soluble PR3 (Dolman et al., 1993; van der Geld et al., 2002). The investigation of a large collection of longitudinally collected samples from patients with GPA ($n = 433$) recently provided evidence for PR3 activity-modulating C-ANCAs (80%). The inhibitory type of C-ANCA was most prevalent, but C-ANCAs with activity-enhancing effects on PR3 were also identified. C-ANCAs with inhibitory capacity partially block PR3 activity by an allosteric mechanism of inhibition (Hinkofer et al., 2013, 2015). Epitope mapping revealed that these mAbs bind mainly to a region that overlaps with that of group 1 (Hinkofer et al., unpublished data).

D. Membrane Binding Area

Unlike other NSPs, PR3 is already expressed at the surface of resting naive neutrophils purified from the peripheral blood. Several groups reported a bimodal cell surface expression pattern of PR3, representing a large population of PR3-positive resting neutrophils and a small subpopulation of PR3-negative resting neutrophils (Halbwachs-Mecarelli et al., 1995). This peculiar

type of distribution is genetically determined (Schreiber et al., 2003). PR3 constitutively expressed on resting neutrophils has been designated "constitutive PR3." It is still unclear how constitutive PR3 is expressed on resting neutrophils. Exposure of neutrophils to cytokines (tumor necrosis factor-α) and chemoattractants (platelet activating factor, formyl-Met-Leu-Pro, or interleukin-8) increases the expression of PR3 at the neutrophil surface (Campbell et al., 2000). PR3 expressed on membranes as a consequence of neutrophil activation has been called "induced PR3" (Korkmaz et al., 2009, 2013b). PR3^m is detected using mouse anti-PR3 mAbs belonging to groups 1, 2, and 3, indicating that the structural determinant recognized by these mAbs (epitopes 1–3) is accessible in PR3^m.

Since membrane expression of PR3 is pivotal for its proinflammatory functions in GPA, the interaction of PR3 with neutrophil surfaces has attracted much attention and has been investigated by several groups. The three-dimensional structure of PR3 shows a closely spaced hydrophobic surface patch (Phe165, Phe166, Ile217, Trp 218, Leu223, and Phe224) and a small cationic cluster (Lys187, Arg186, Arg186B, and Arg222) on the C-terminal β-barrel (Fujinaga et al., 1996). PR3^m is not solubilized in high-salt buffers, indicating that electrostatic interactions are not involved in its membrane interaction (Korkmaz et al., 2009). This has been taken as an indication for the hydrophobic nature of PR3^m binding. The hydrophobic patch of human PR3 is not conserved in mammals (Korkmaz et al., 2008a). Except for chimpanzees, three of the hydrophobic residues (namely, Phe166, Trp218, and Leu223) are substituted by charged or polar residues (e.g., on the surface of mouse and other primates). A human–gibbon (*Hylobates pileatus*) PR3 chimera with a gibbon C-terminal β-barrel, which differs only by nine residues from human PR3, cannot interact with human NB1 and cellular cell surfaces in vitro (Korkmaz et al., 2008a). In addition, PR3 is not found on the surface of quiescent neutrophils from mice (Pfister et al., 2004) and macaques (Korkmaz et al., unpublished data). These data collectively led to the conclusion that the unique solvent-accessible hydrophobic patch of PR3 mediates its membrane interaction. More recently, Kantari et al. (2011) reported that the mutation of four hydrophobic residues of this patch (Phe165, Phe166, Leu223, and Phe224) prevented PR3 expression on rat basophilic leukemia-1 cells.

Because the hydrophobic patch is part of the activation domain that changes, upon zymogen conversion, the active PR3, and not so much its zymogen, can bind to the surface of NB1-transfected HEK293 cells (von Vietinghoff et al., 2007) and Chinese hamster ovary cells (Korkmaz et al., 2008a). Group 5 mouse anti-PR3 mAb MCPR3-7, which preferentially binds to the activation domain of the zymogen, prevents the binding of PR3 to cellular membranes expressing human NB1 after

transfection (Korkmaz et al., unpublished data). When MCPR3-7 was used for the detection of PR3^m on resting or activated neutrophils, none of the cells displayed PR3 binding to this antibody, indicating that the hydrophobic patch of the activation domain is involved in membrane binding (Silva et al., 2010). Taken together, these results support the hydrophobic nature of PR3 membrane interactions.

IV. Protein and Chemical Inhibitors of Proteinase 3

A. Protein Inhibitors

1. Serine Protease Inhibitors. Serine protease inhibitors (serpins) are the largest and most diverse superfamily of protease inhibitors, containing between 350 and 500 amino acid residues with molecular weights ranging from 40 to 60 kDa (Gettins, 2002). Over 3000 members of the serpin superfamily have been identified in animals, plants, bacteria, archaea, and viruses (Irving et al., 2000; Silverman et al., 2001; Mangan et al., 2008; Olson and Gettins, 2011). They can operate in intracellular and extracellular environments (Silverman et al., 2001; Gettins, 2002). Serpin members have been classified into 16 clades (A–P) based on their evolutionary relationships. Most human serpins belong to clades A and B, which form gene clusters on chromosome 14 and on chromosomes 6 and 18, respectively. In mammals, a large group of serpins in plasma regulate serine protease cascades of the complement and blood coagulation and fibrinolysis systems (Olson and Gettins, 2011). Serpins, which are single-chain proteins, share a similar, highly conserved tertiary structure. The consensus fold of a native serpin contains three β-sheets (termed sA–sC) and eight or nine α-helices (termed hA–hI) and possesses a reactive center loop (RCL) (Fig. 5A). The RCL is a solvent-exposed flexible stretch of 20 to 21 amino acid residues positioned between β-sheets sA and sC and adopts a metastable, so-called stressed conformation in native inhibitory serpins.

Most serpins can be classified as a mechanism-based "suicide" or "single-use" inhibitor because the RCL is attacked by the target protease between P1 and P1′ and forms a stable covalent enzyme-inhibitor complex (Huntington et al., 2000). The P1 residue in the RCL is critical for the specificity of a serpin toward a particular protease (Jallat et al., 1986). X-ray crystal structures of encounter complexes, which are serpins bound to a catalytically inactive protease, reveal that the RCL acts as a pseudosubstrate for the respective target protease in the canonical conformation (Dementiev et al., 2003) (Fig. 5B). Initially, the RCL binds to the target protease active site by reversible noncovalent association, which is the rate-limiting step of the entire inhibitory reaction (Gettins, 2002). This noncovalent reversible Michaelis complex is then converted into an acyl-enzyme
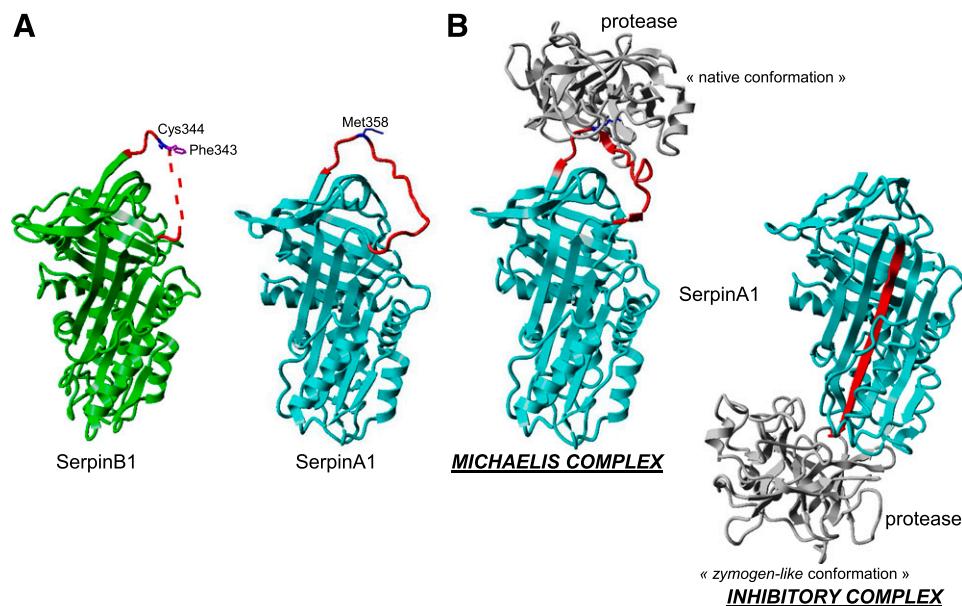
Fig. 5. X-ray crystal structure of native serpins and serpin protease complexes. (A) Ribbon representation of serpinB1 (MNEI) (PDB code 4GA7) and serpinA1 (α1PI). The P1 residues are shown in stick representation. (B) Ribbon representation of the noncovalent complex of S195A trypsin with α1PI Pittsburgh (PDB code 1POH) (left). Ribbon representation of the covalent complex of α1PI with pancreatic elastase (PDB code 2D26) (right). The exposed and inserted RCLs are in red. PDB, Protein Data Bank.

intermediate, in which the target protease is covalently linked to the serpin by an ester bond formed between the Ser195 oxygen of the protease and the P1 carbonyl carbon of the RCL loop (Fig. 5B). An approximately 4-kDa C-terminal fragment generated after the cleavage of the RCL by the protease remains noncovalently bound to the cleaved serpin. The RCL linked to the protease inserts into β-sheet sA of the serpin, dragging the protease with it. This inhibitory pathway results in a 71-Å translocation of the protease to the opposite site of the serpin and the formation of a hyperstable six-stranded A-sheet conformation. In the 1:1 stoichiometric (enzyme/inhibitor) covalent inhibitory complex, the oxyanion hole of the protease bound to the serpin is distorted (Olson and Gettins, 2011). This structural rearrangement abrogates the catalytic mechanism of the protease and prevents the hydrolysis of the acyl complex (Huntington et al., 2000; Dementiev et al., 2006). The structural alterations of the protease in particular pertain to the activation domain loops of the protease, which adopt a zymogen-like conformation (Huntington et al., 2000; Dementiev et al., 2006) (Fig. 5B). The initial encounter complex between the serpin and its target protease may result in cleavage of the RCL without subsequent formation of the covalent complex (Olson and Gettins, 2011). This substrate pathway depends on the nature of the serpin and the protease. It results in the formation of an RCL-cleaved serpin and release of an active enzyme. The substrate pathway increases the inhibitor/enzyme ratio for full inhibition, which is often higher than 1.

The transfer of the serpin RCL or part of it into another serpin does not generally result in the transfer of the inhibitory specificity. The resulting chimeric serpin often behaves like a substrate and is cleaved by target proteases without forming the covalent complex. By contrast, single-residue substitutions within RCLs and usually that of the P1 residue have been utilized to change the inhibitory specificity of serpins (Jallat et al., 1986).

a. α-1 Protease inhibitor. For historical reasons, α1PI was first named α-1-antitrypsin because it was found to inhibit pancreatic trypsin. This archetypal member was assigned the first number of the clade A (serpinA1). Later, it was shown to inhibit a wider range of serine proteases, including NSPs, and it was thus renamed α1PI. The largest proportion of the mature polypeptide chain is produced by the liver and secreted as a 52-kDa sialoglycoprotein (394 residues) into the blood (Janciauskiene, 2001). It is the second most abundant plasma protein after albumin/IgG, with circulating levels between 1.2 and 2 mg/ml (20–40 μM) in healthy individuals (Jeppsson et al., 1978; Crystal et al., 1989). The α1PI gene named *SERPINA1* is localized on the long arm of chromosome 14 (14q32.1).

The exposed RCL of α1PI is cleaved at the Met358 to Ser359 bond (P1–P1′) upon interaction with target proteases (Table 3). The X-ray structure of free α1PI revealed that its RCL adopts a canonical-like conformation from Pro361 to Ile356 (P3′–P3), with an extension as a β-pleated strand from Ile356 to Met351 (P3–P8). This rigid canonical conformation of RCL is stabilized by intramolecular contacts (Elliott et al., 1996). α1PI is an efficient inhibitor of HNE with a second-order association rate constant (k_{ass}) of 6.5×10^7 M^{-1}s^{-1} and an inhibitor/enzyme stoichiometry index (SI) of 1 (Beatty et al., 1980). However, the k_{ass} of α1PI is 100 times less

TABLE 3
Protein inhibitors blocking human PR3 activity
Boldface represents reactive center loop residues. Underlining represents substitutions.

Inhibitor	Reactive Center Sequence	Rate Constant		Reference
		PR3	HNE	
Serpins, k_{ass} (M^{-1}s^{-1})				
α1PI	GTEAAGAMFLEAIP**M S**IPPE	4.5×10^5	6.5×10^7	Epinette et al., unpublished data; Beatty et al., 1980 for PR3 and HNE, respectively
ACT(IPM/SIP)	GTEASAATAVKI**IPM SI**PVE	1.9×10^5	1.0×10^6	Groutas et al., 1997
SerpinB1	GTEAAAATAGIA**TFC M**LMPE	3×10^4	3.4×10^7	Jégot et al., 2011 and Cooley et al., 2001 for PR3 and HNE, respectively
SerpinB1(STDA/R)	GTEAAAATAGI**S**T**DA R**LMPE	1.4×10^7		Jégot et al., 2011
Canonical inhibitors, K_i (M)				
Elafin	LIRC**A ML**	1.2×10^{-10}	0.8×10^{-10}	Zani et al., 2004
Elaf-SLPI2	LIRC**A ML**	7.6×10^{-11}	2.2×10^{-11}	Zani et al., 2009
SLPI2-Elaf	LIRC**A ML**	43×10^{-11}	5.2×10^{-11}	Zani et al., 2009
Trappin-2	LIRC**A ML**	1.8×10^{-10}	0.3×10^{-10}	Zani et al., 2004
Trappin-2 A62L	LIRC**L ML**	3.7×10^{-9}	1.5×10^{-11}	Zani et al., 2009
α2-M, k_{ass} (M^{-1}s^{-1})	39-residue bait region: Pro690-Thr728	1.1×10^7	4.1×10^7	Rao et al., 1991 and Virca and Travis, 1984 for PR3 and HNE, respectively
Antibodies, K_i (nM)				
MCPR3-7	Binding site: ScFv	N.I.		
hAb-EI-L7	Binding site: TSVHQET-MCT**A S**IPPQCY-YEWHVDV	>300	0.83	Liu et al., 2015

ACT, antichymotrypsin; N.I., not identified.

for PR3 ($k_{\mathrm{ass}} = 4.5 \times 10^5$ M^{-1}s^{-1}) (Epinette et al., 2012) than for HNE (Sinden et al., 2015; Epinette et al., unpublished data) and the SI is approximately 1.3 because of proteolytic inactivation of some α1PI molecules occurring in the course of interaction (Korkmaz et al., 2005b). α1PI contains a P1 methionine residue Met358 in its RCL, which can be oxidized in vitro by reactive oxygen species or activated neutrophils. Oxidation of this residue results in a marked loss of inhibition of NSPs by α1PI. The substitution of the Met by a Val makes this α1PI(Met358/Val358) variant resistant to oxidizing agents (Courtney et al., 1985). Moreover, it does not inhibit trypsin or other plasma serine proteases with trypsin-like specificity (Travis et al., 1985). Other α1PI variants with alanine, cysteine, leucine, or isoleucine at position 358 were produced (Jallat et al., 1986; Matheson et al., 1986). They are all potent inhibitors of HNE and are resistant to oxidation. A genetically engineered hybrid antichymotrypsin containing P3–P3′ residues of α1PI, called LEX032, is an efficient inhibitor of PR3 (Groutas et al., 1997).

More than 100 genetic variants of α1PI with amino acid substitutions or deletions have been reported (Salahuddin, 2010). At the protein level, these natural α1PI variants exhibit different isoelectric focusing behavior in the pH range of 4 to 5 and are distinguished by a capital letter (M, S, or Z) according to their isoelectric focusing position. The most common normal variants (approximately 50) migrate in the middle region and are assigned an M. S and Z α1PI variants are identified as more cathodal variants because of a positive charge increase, with Z migrating most cathodal. The S (Glu264Val) and Z (Glu342Lys) variants carry a single amino acid substitution. The majority of patients are homozygous for the Z variant, which is

frequent in Northern European (allele frequency 1 in 27) and Polish individuals. Compound heterozygotes—particularly in combination with S, a frequent allele (1 in 8) in the population of the Iberian Peninsula—and null alleles in combination with a single Z allele have been reported and are probably under-recognized. Abnormalities of these two variants result in decreased or undetectable α1PI levels in serum. Levels below 35% are associated with an increased risk of pulmonary emphysema, GPA, and liver diseases. α1PI deficiency affects approximately 1 in 2000–5000 individuals. S and Z variants function normally as HNE inhibitors and their k_{ass} values for HNE are almost the same as those of normal α1PI.

In addition to common S and Z variants, several rare deficiency variants for α1PI have been reported (Salahuddin, 2010). An α1PI variant with an Arg at position 358, replacing the normal P1 methionine, was identified in the plasma of a 14-year-old boy who died from a fatal bleeding disorder (Owen et al., 1983). This natural variant, called Pittsburgh α1PI, is a potent inhibitor of thrombin, plasmin, and plasma kallikrein and acts as an uncontrolled anticoagulant. It has 10^4-fold decreased k_{ass} for HNE. This finding indicates that the reactive center of α1PI is methionine 358, which acts as "bait" for HNE (Schapira et al., 1986; Scott et al., 1986). The X-ray structure of Pittsburgh α1PI noncovalently bound to trypsin was identified using a bovine trypsin variant in which the Ser of the catalytic triad was replaced by Ala at position 195 (Dementiev et al., 2003) (Fig. 5B). The crystal structure revealed that the RCL loop of Pittsburgh α1PI did not change upon binding with S195A trypsin. The contact area was located between P2 and P2′. These data suggested a limited canonical-like interaction between α1PI and its

target protease in the Michaelis complex. Our preliminary data show that the Pittsburgh α1PI variant forms a reversible complex with PR3 (Korkmaz and Jenne, unpublished data).

b. Monocyte neutrophil elastase inhibitor. The monocyte neutrophil elastase inhibitor (MNEI), also called serpinB1, is a cytoplasmic serpin without carbohydrates and a signal peptide. It belongs to clade B and is also named the ov-serpin family, meaning ovalbumin-related serpins. Members of clade B are characterized by a high homology to chicken ovalbumin, which lacks protease inhibitory activity (Hunt and Dayhoff, 1980; Benarafa and Remold-O'Donnell, 2005). The human *SERPINB1* gene is located on chromosome 6 (Zeng et al., 1998). SerpinB1 is highly expressed in the cytosol of neutrophils and monocytes (Remold-O'Donnell et al., 1989).

Unlike α1PI, serpinB1 displays two functional reactive sites in the RCL, one at Phe343-Cys344 and the other at Cys344-Met345 (Table 3), either of which can be cleaved by target proteases. Phe343 and Cys344 act as the P1 residue, respectively, for serine proteases with chymotrypsin-like (e.g., CatG and chymase) and elastase-like (e.g., PR3 and HNE) specificities (Cooley et al., 2001). SerpinB1 inhibits PR3 ($k_{ass} = 3 \times 10^4$ M^{-1}s^{-1}) with a SI close to 1 (Jégot et al., 2011). The first selective inhibitor of PR3 over HNE and CatG was derived from serpinB1. The dual inhibition of serine proteases with chymotrypsin- or elastase-like specificities seems to be linked to the greater flexibility of the serpinB1 RCL. Thus, inhibition of target proteases should not be significantly altered by replacing a few residues within the flexible RCL. We explored the structural differences between PR3 and HNE active sites to generate a recombinant serpinB1 called serpinB1 (STDA/R), which contains only four substitutions in its RCL (Jégot et al., 2011). The substitution of P2 residue Phe343 by Asp abolished the interaction and cleavage by CatG, whereas it improved the interaction with the S2 residue Lys99 of PR3. The Asp-Ala-Arg sequence in peptide substrates is selectively and efficiently cleaved by PR3 over HNE at the Ala-Arg bond, which explains the choice of these residues from P2 to P1′. Ala341 has been substituted by a Ser residue at P4 to prevent the processing by HNE. Despite the presence of an Asp-Ala-Arg sequence in the RCL, the variant serpinB1(STDA/R) was cleaved by HNE at the Ala-Arg bond without irreversible trapping. SerpinB1(STDA/R) is an efficient inhibitor of PR3, with a second-order association rate constant of 1.4×10^7 M^{-1}s^{-1} and an SI below 2. The k_{ass} is approximately 100 times faster than that observed for wild-type serpinB1 and is similar to that of the α1PI for HNE. Like α1PI, SerpinB1(STDA/R) inhibited and removed the induced PR3^m from the membranes of activated neutrophils (Jégot et al., 2011).

The three-dimensional structure of serpinB1 was recently identified by Wang et al. (2013) in the native conformation using a RCL variant in which Leu346 and Met347 were mutated to Asp (Protein Data Bank code 1BY7) (Fig. 5A). The serpinB1 structure contains three β-sheets, nine α-helices, and a flexibly exposed RCL. In the crystal, two serpinB1 molecules are linked together by a disulfide bond between Cys344 of the RCL. In the dimer, the P residues ranging from 332 to 341 of chain A and from 330 to 341 in chain B lack clear electron density, because they are disordered and not visible. P′ residues are, however, visible with well defined electron densities. These findings are a further indication for the high flexibility of the RCL in serpinB1.

2. Canonical Inhibitors. Canonical inhibitors that represent the largest group of protein inhibitors are found in high quantities in plant seeds, avian eggs, and various body fluids. Canonical inhibitors composed of 14 to approximately 200 amino acid residues are grouped into 18 families (e.g., Kazal, Bowman-Birk inhibitor, chelonianins), which all display a different fold but share a similar protease-interacting segment called the protease-binding loop. In all known members, this convex and solvent exposed loop adopts a canonical conformation that is complementary to the concave active site of the target protease. Their protease-binding loop in the P3–P3′ region acts like an optimal substrate, forming an enzyme-inhibitor complex. This noncovalent main chain interaction via antiparallel β-pleated strands between the inhibitor and protease resembles the protease-substrate Michaelis complex. Upon binding, the reactive site P1–P1′ can be selectively hydrolyzed by the target protease. However, the catalytic rate constant for the hydrolysis of the reactive site is extremely low at neutral pH. The mode of recognition between different canonical inhibitors and target serine proteases is always almost the same and follows the standard mechanism (Laskowski and Kato, 1980; Krowarsch et al., 2003).

Elafin and SLPI are two inhibitors that belong to the chelonian family. These proteins are identified as alarm antiproteases because they are locally produced during infection. They are the best characterized inhibitors of the chelonian family and are able to inhibit NSPs. In addition to their inhibitory properties, they possess broad-spectrum antimicrobial activities (Sallenave, 2010; Scott et al., 2011).

a. Elafin. Elafin, also called skin-derived antileukoprotease, is an alarm antiprotease that has been isolated from the skin of patients with psoriasis (Schalkwijk et al., 1990; Wiedow et al., 1990) and from the sputum of patients with COPD (Sallenave and Ryle, 1991; Sallenave et al., 1992). Elafin is synthetized as a 9.9-kDa full-length pre-elafin precursor (also called trappin-2, which is an acronym for transglutaminase substrate and wAP domain containing protein). The unglycosylated 95-residue cationic pre-elafin is composed of an N-terminal "cementoin" domain (38 residues) and a C-terminal globular inhibitory WAP

domain (57 residues) (Nara et al., 1994). The N-terminal domain contains several repeats of a motif that facilitates the transglutaminase-mediated anchoring of pre-elafin to extracellular matrix components. The three-dimensional structure of elafin with the C-terminal inhibitory domain was crystallized in a complex with porcine pancreatic elastase (Tsunemi et al., 1996). It is stabilized by four disulfide bridges characteristic of whey acidic proteins. The inhibitory loop is constituted by the residues Leu20 to Leu26. Its C-terminal inhibitory domain shares approximately 40% identity with the SLPI inhibitory domain. Mast cell tryptase has been identified as the protease that releases the 6-kDa elafin domain from its precursor (Guyot et al., 2005). The elafin gene protease inhibitor 3 (PI3) is constitutively expressed in several epithelial cells, including the skin, lungs (Vos et al., 2005), oral cavity, and vagina (King et al., 2003). Elafin is synthesized by bronchial and epithelial cells of the respiratory tract. Its concentration in bronchial secretions of normal subjects ranges from 1.5 to 4.5 μM (Tremblay et al., 1996; Ying and Simon, 2001).

Recombinant elafin and its precursor produced in *Saccharomyces cerevisiae* and in *Pichia pastoris* expression systems have identical high affinities for PR3 and HNE. The K_i values determined by different groups are in the 10^{-10} M range (Table 3). Elafin interacts with target proteases via the Ala24-Met25 segment, which contains an oxidizable Met at the P1' position. Oxidation of elafin and its precursor lowers their affinities for PR3 and HNE. Substituting P1' Met with Leu in elafin and its precursor abolishes inhibition of PR3, while slightly decreasing the affinity of both inhibitors for HNE (Nobar et al., 2005). Elafin/pre-elafin can inhibit PR3^m and HNE^m at the surface of activated neutrophils. Elafin-PR3^m complexes remain bound on the neutrophil cell surface (Korkmaz et al., 2009).

b. Secretory leukocyte protease inhibitor-elafin chimeras. SLPI is a nonglycosylated highly basic 107–amino acid single-chain protein that has been initially isolated from bronchial secretions (Hochstrasser et al., 1972; Ohlsson and Tegner, 1976). It is found in all body fluids, including urine, tears, salivary glands, seminal fluids, and cervical and intestinal mucus. SLPI concentrations are estimated to be around 9 μM in bronchial secretions of normal subjects (Vogelmeier et al., 1997). The crystal structure of SLPI in the complex with bovine chymotrypsin reveals two homologous domains each containing four disulfide bridges (Grütter et al., 1988). Only the C-terminal domain is involved in protease binding. The Leu72-Met73 dipeptide has been identified as the P1–P1' residues. SLPI is a high affinity canonical inhibitor of HNE, with a K_i of 0.1×10^{-10} M (Gauthier et al., 1982), but it does not inhibit PR3 significantly. The lack of PR3 inhibition by SLPI is explained by the reduced size of the S1 pocket of PR3 impairing the accommodation of P1 Leu72. Lack of a

hydrogen bound around the PR3 S5 pocket (Koizumi et al., 2008) and unfavorable charge contacts between PR3 and SLPI (Zani et al., 2009) were also reported to explain the lack of PR3 inhibition by SLPI.

Zani et al. (2009) produced two recombinant SLPI-elafin chimeras in *P. pastoris*. In the first chimera, they replaced the noninhibitory N-terminal domain of SLPI with the elafin domain to give elaf-SLPI2. In the second chimera, named SLPI2-elaf, the elafin domain was fused to the C-terminal side of SLPI2. Both mutants were reported to strongly interact with PR3, HNE, and CatG, with K_i values in the 10^{-11} range (Table 3). The SI for both chimeras has been determined and amounts to 1:1 for PR3 and 2:1 for HNE.

3. α-2-Macroglobulin. Human α-2-macroglobulin (α2-M) is an abundant 725-kDa homotetrameric plasma protease inhibitor synthesized in the liver (Barrett and Starkey, 1973; Travis and Salvesen, 1983; Sottrup-Jensen, 1989). It is present at a concentration of 2 mg/ml in serum (Petersen, 1993). Because of its high molecular mass, it cannot readily diffuse to inflammatory sites during neutrophil extravasation, and therefore controls protease activities primarily within the circulation. α2-M displays broad inhibitory specificity and inhibits all four major classes of proteases that form a 1:1 or 2:1 complex with tetrameric α2-M (Travis and Salvesen, 1983; Sottrup-Jensen, 1989). Marrero et al. (2012) recently demonstrated that α2-M operated through a unique irreversible "venus flytrap" mechanism, which "entraps" target proteases in the inhibitor tetramer. Proteases are captured and trapped by conformational changes occurring after the cleavage of a multitarget "39-residue bait region" (Pro690-Thr728) by the protease (Barrett and Starkey, 1973; Sottrup-Jensen, 1989). The α2-M mechanism of interaction with target proteases has been described in detail (Marrero et al., 2012; Garcia-Ferrer et al., 2015). Its covalent association with proteases sterically shields their active sites from large molecular substrates, permitting enzymatic hydrolysis of only small synthetic substrates (Doan and Gettins, 2007). α2-M inhibits PR3, with a second-order association rate constant of 1.1×10^7 M^{-1}s^{-1} (Rao et al., 1991). The cleavage site of PR3 within the bait region has not been identified.

4. Antibodies Interfering with Activity. mAbs, which show a relatively long half-life, high affinity, and selective binding, are regarded as therapeutic agents for a variety of human diseases. Moreover, antibodies that interfere with the catalytic activity of serine proteases have been generated. To identify antibodies with protease-inhibiting properties, different approaches involving immunization or screening of the phage display of combinatorial antibodies libraries have been explored. The mAbs generated have been classified into two groups (Ganesan et al., 2010). The first group of antibodies inhibits protease activity by hindering substrate access to the catalytic cleft, whereas the

second group induces an allosteric switch mechanism. The first group of antibodies can bind close to or within the substrate binding region of the target protease. This binding is mediated by the complementary determining regions of the antibody in a way that substrate access to the catalytic cleft is partially or fully occluded. The second group of antibodies does not directly interact with the substrate binding site of the target antigen. The epitopes of this group are located at the periphery of the substrate binding region. Upon binding, mAbs of this group alter the conformation of loops surrounding the substrate binding pockets, which results in reduced or suppressed catalytic activity of the target protease toward an extended peptide substrate.

MCPR3-7 is a monoclonal mouse anti-PR3 antibody that can interfere with the catalytic activity of PR3 by an allosteric mechanism (Hinkofer et al., 2013). Initially, this mAb was generated to discriminate between proteolytically active mature PR3 and its inactive zymogen, which displays a different conformation. For the generation of a mAb with preferred binding to the PR3 zymogen, BALB/c mice were immunized with a purified N-terminally protected pro-PR3 variant. The latter was produced with the amino-terminal sequence AEP-I$_{16}$ in nonhematopoietic HEK293 cells. A proline residue was inserted between the natural propeptide Ala-Glu-Pro-Ile16 and the amino terminus of mature PR3 to prevent the processing by exopeptidases. The clone called MCPR3-7 preferably bound to the PR3 zymogen in direct comparison with the mature PR3 in a capture enzyme-linked immunosorbent assay. The PR3 zymogen in solution had a 40-fold higher affinity for MCPR3-7 than mature PR3, as determined by thermophoresis. MCPR3-7 also showed much stronger binding to the covalent PR3-α1PI complex than to the canonical PR3-α1PI complex. In the covalent PR3-α1PI complex, PR3 has a zymogen-like conformation that increases its affinity for MCPR3-7 (Hinkofer et al., 2013).

MCPR3-7 completely reduces the proteolytic activity of mature PR3 at a 3-fold molar excess toward synthetic extended FRET substrates. In PR3–MCPR3-7 complexes, the shape and/or access to the PR3 S1′ subsite is primarily altered. However, the major binding region of MCPR3-7 is located in the activation domain of the PR3 zymogen. Binding of MCPR3-7 to the proform of PR3 induces little conformational change of the zymogen (Fig. 6). By contrast, the interaction of MCPR3-7 with mature PR3 forcefully induces this zymogen-like catalytically inactive state even after the removal of the propeptide by CatC. This zymogen-like inactive conformation of mature PR3 occurs with low probability in solution and is in equilibrium with the highly favored active conformation of mature PR3. The binding of MCPR3-7 to the zymogen-like conformation of mature PR3 shifts the equilibrium toward the inactive PR3 with its modified substrate binding cleft (Fig. 6). Inhibition of PR3 activity is most likely due to an allosteric effect

altering the conformations of the autolysis and 187–190 loops located around S1, S1′, and S2′ subsites. The binding of MCPR3-7 to PR3 also affects the covalent or canonical complexation with α1PI and delays the irreversible inhibition of PR3. MCPR3-7 is the first prototype of a PR3-directed conformation specific mAb with inhibitory properties (Hinkofer et al., 2013).

Liu et al. (2015) recently developed a novel strategy to design antibody-based inhibitors with nanomolar affinities for serine proteases with a trypsin-like fold (bovine trypsin and HNE) by engineering the exceptionally long CDR3H loop of a subgroup of bovine antibodies. The X-ray crystal structure of one such antibody showed a highly solvent exposed novel structure in which the elongated CDR3H loop folds into a disulfide-linked distal "knob" domain attached to the evolutionary conserved, antiparallel β-strand "stalk." The latter is common to canonical serpin families. By inserting the active β-hairpin loop of sunflower trypsin inhibitor-1 into the CDR3H β-strand stalk of a bovine antibody, trypsin-inhibiting Fabs have been generated. Anti-HNE Fabs have been engineered by inserting a known disulfide-bridged HNE-inhibiting peptide (McBride et al., 1999) into the β-strand "stalk," whose length was varied and reduced from nine to seven residues. These Fabs were then humanized. The anti-HNE Fab called hAb-EI-L7 (the human anti-elastase inhibitory antibody with a β-strand linker is seven residues in length) is a potent HNE inhibitor ($K_i = 0.83 \pm 0.31$ nM). hAb-EI-L7 weakly inhibits PR3, with a $K_i > 300$ nM, and is therefore more than 300-fold more potent toward HNE (Liu et al., 2015).

B. Synthetic Inhibitors

1. Substrate-Like Pseudopeptide Inhibitors. Pseudopeptides are peptide derivatives with an altered chemical structure that prevents degradation or modifications by endogenous enzymes. Pseudopeptides include azapeptides, amide bond surrogates, and peptoids. Azapeptides are peptide analogs in which one or more α-carbon atoms have been replaced by a nitrogen atom (Proulx et al., 2011). They can act as protease inhibitors when the replacement affects the α-carbon of the P1 residue in peptide analogs (Adessi and Soto, 2002; Zega, 2005). Azapeptides for the use as protease inhibitors generally contain a P1 aza–amino acid residue and a good reactive leaving group (-ONp, -OCH$_2$CF$_3$, -OPh), so that they form with the target protease a stable acyl-enzyme intermediate that dissociates very slowly (Zega, 2005). The substitution of a carbon by a nitrogen atom at P1 decreases the electrophilicity of the P1 carbonyl group and also moves the geometry of the complex away from a tetrahedron. The acyl derivative is a carbazate and is much more stable toward nucleophilic attack by water than the ester formed with substrates. The majority of azapeptides that inhibit serine proteases, including HNE, are
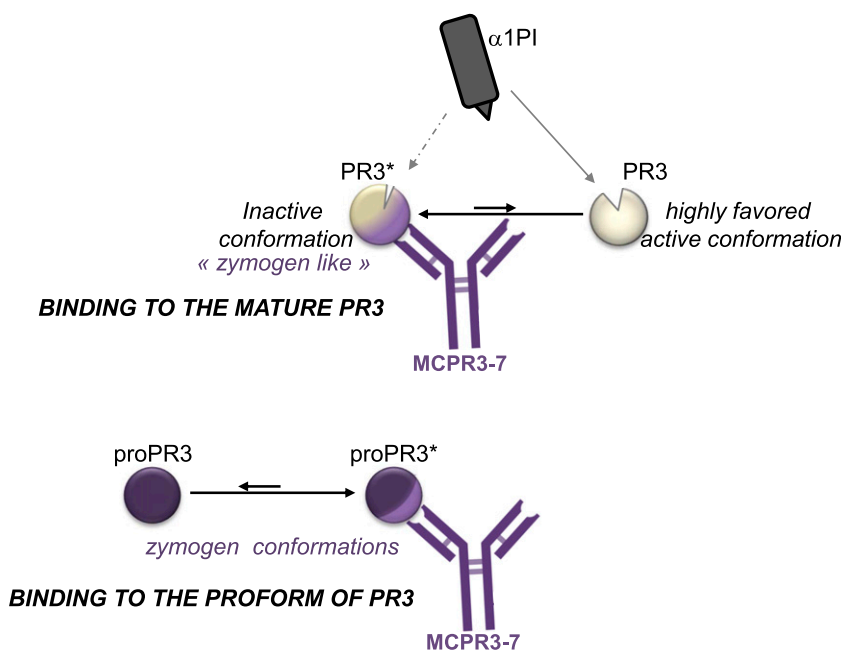
Fig. 6. Interaction of mAb MCPR3-7 with PR3. Binding of MCPR3-7 to the proform of proteinase 3 (proPR3) leads to slight conformational modification of the zymogen (bottom). The mature form of PR3 occurs in an equilibrium between a highly favored active (open substrate binding cleft; right shape) and zymogen-like inactive conformation (modified substrate binding cleft; left shape). Interaction of MCPR3-7 shifts the equilibrium toward zymogen-like inactive conformation and stabilizes this altered conformation displaying modified activity and substrate specificity. Binding of MCPR3-7 to the zymogen-like inactive conformation has an inhibitory effect on the complexation with α1PI (dotted arrow).

peptide-nitrophenyl esters that release 4-nitrophenol when the acyl-enzyme complex is formed (Powers et al., 1984; Zega, 2005). Azapeptides containing a poor leaving group cannot acylate target proteases but simply act as reversible inhibitors (Dorn et al., 1977).

Recently designed azapeptide inhibitors have a peptide chain on their P′ side and bind to the protease noncovalently and reversibly (i.e., without acylation or deacylation) (Zhang et al., 2002). Their affinity for the protease active site is similar to that of the substrate, and the K_i value is much like the K_m of the parent substrate. The first synthetic PR3 inhibitor was derived from the selective PR3 FRET substrate ABZ-VADnorVADYQ-Y(NO$_2$) (M_r = 1206 Da) and had a low K_m of 1.2 μM (Epinette et al., 2012). The α-carbon of the P1 residue (norVal) in the peptide moiety was replaced by a nitrogen atom (Fig. 7, A and B). Otherwise, the peptide sequence and the fluorescence donor/acceptor pair (ABZ = Tyr$_{NO_2}$) was not altered to maintain the water solubility and features as a FRET substrate. The resulting azapeptide ABZ-VAD(aza)norVADYQ-Y(NO$_2$) (M_r = 1207 Da), called azapro-3 differs from the parent substrate only by 1 Da. Azapro-3 does not form a stable acyl-enzyme complex with PR3, as shown directly by native mass spectrometry and indirectly by the absence of an increase in fluorescence that would result from the cleavage of the peptide backbone. Thus, azapro-3 is a reversible competitive inhibitor, with a K_i of 1.5 μM comparable to the K_m of the parent substrate. Azapro-3 inhibits PR3 in solution, PR3^m, and also the PR3 present in biologic samples. It does not inhibit neutrophil

HNE to any significant extent and does not inhibit CatG, chymotrypsin, or granzyme B. Azapro-3 is highly stable in a lysate of neutrophils and in bronchial lavage fluids of patients with neutrophilic pulmonary diseases. The inhibitor was significantly degraded only after it had been incubated with purified PR3 for at least 24 hours; it was cleaved at a single site, P1–P1′ [(aza)norV-A], in these conditions. This degradation was so slow that it did not interfere with the almost immediate inhibition produced by inhibitor concentrations in the 10-μM range. Finally, azapro-3 did not alter the viability of a suspension of purified neutrophils, even after incubation with the inhibitor for several hours, and the inhibitor did not enter the cells (Epinette et al., 2012).

Amide bond surrogates are pseudopeptides in which some amide bonds have been replaced by other chemical groups. The psi-bracket ([Ψ]) is used as the nomenclature for these replacements (Adessi and Soto, 2002). The introduction of such modifications in the peptidyl sequence completely blocks protease-dependant cleavage of the amide bond. This modification may also alter the conformation and the flexibility of the peptides. Budnjo et al. (2014) recently developed amide bond surrogates in which the scissile amide bond CONH is replaced with a COCH$_2$ between norVal and Ala (Fig. 7C) in the selective PR3 FRET substrates Abz-VADnorVADYQ-EDDnp and Abz-VANnorVAERQ-EDDnp (Table 4). The synthesis was made possible by incorporation of a norVal-Ala ketomethylene dipeptide isostere in peptidyl sequences in place of the norVal-Ala. The resulting amide bond surrogates Abz-VADnorV[Ψ](COCH$_2$)-ADYQ-EDDnp

A   **ABZ-VADnorVADYQ-Y(NO2)**

B   **ABZ-VAD(aza)norVADYQ-Y(NO2)**
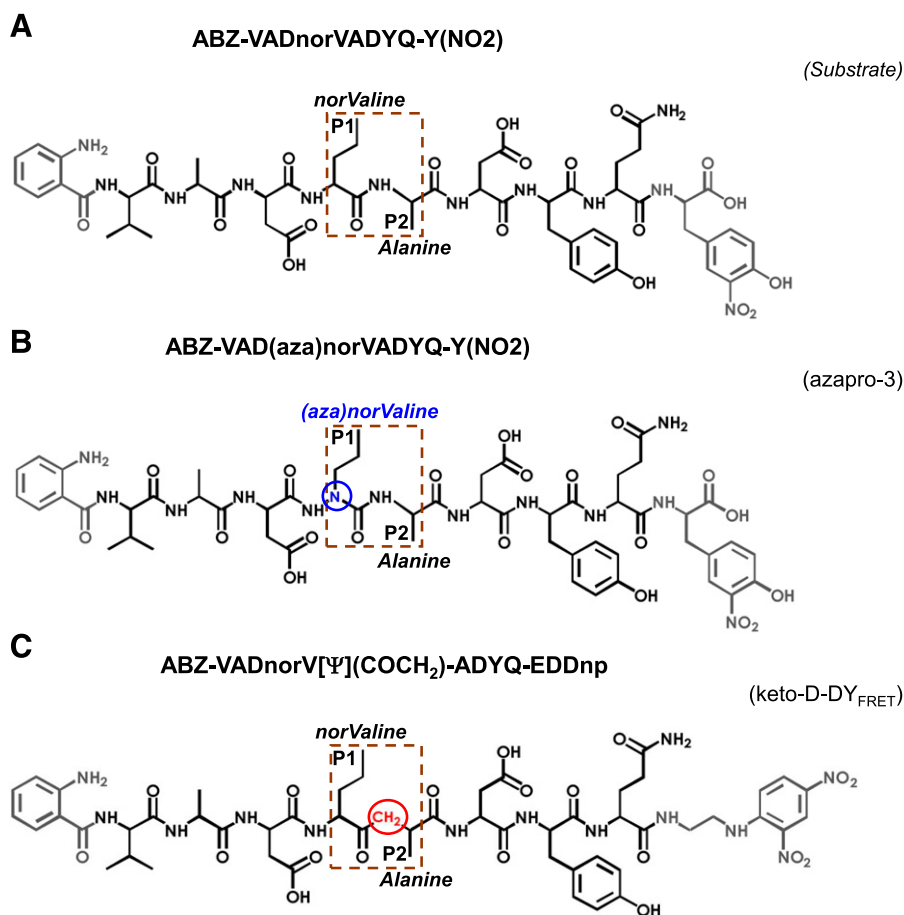

C   **ABZ-VADnorV[Ψ](COCH₂)-ADYQ-EDDnp**

Fig. 7. Chemical structures of substrate-like pseudopeptide inhibitors of PR3. (A) Structure of parent PR3 substrate ABZ-VADnorVADYQ-Y (NO₂) (Korkmaz et al., 2007). (B) Azapeptide inhibitor of PR3, ABZ-VAD(aza)norVADYQ-Y(NO₂) (azapro-3) (Epinette et al., 2012). The α-carbon of norVal in the parent substrate is substituted by a nitrogen atom. (C) Ketomethylene-based inhibitor of PR3, ABZ-VADnorV[Ψ] (COCH₂)-ADYQ-EDDnp (keto-D-DY_FRET) (Budnjo et al., 2014). norVal-Ala in the parent substrate is replaced by norVal-Ala ketomethylene dipeptide isostere.

and Abz-VANnorV[Ψ](COCH₂)-AERQ-EDDnp are called keto-D-DY_FRET and keto-N-ER_FRET, respectively. These ketomethylene-based inhibitors differ from the parent substrates only by 3 Da and are able to inhibit selectively PR3 over HNE. They display a competitive and reversible inhibition mechanism. Molecular dynamics simulations showed that these peptidomimetic inhibitors display similar interactions with the ligand binding site of PR3 as parent substrates. K_i values of 1.7 μM and 9.1 μM are estimated for keto-D-DY_FRET and keto-N-ER_FRET, respectively (Table 4). The estimated K_i value of keto-D-DY_FRET is almost the same as that of the azapro-3 with a similar peptidyl sequence (Epinette et al., 2012).

Peptoids are a class of peptidomimetics whose side chains are attached to the nitrogen atom of a glycyl peptide backbone, rather than to the α-carbons of amino acids (Zuckermann, 2011). This confers strong resistance to proteolysis and allows a much wider diversity of the side chains than that provided by the 20 amino acids usually found in peptide chains. Peptide-peptoid inhibitors targeting bovine trypsin and chymotrypsin have been synthesized (Stawikowski et al., 2005), but none

has been developed thus far to inhibit PR3 or related NSPs.

2. Transition State Analogs. Transition state analogs are compounds that form transition-state-resembling complexes with serine proteases. The tetrahedral intermediate is formed upon the nucleophilic attack of the Ser195 on the ketone carbonyl of the inhibitors. The tetrahedral intermediate is stabilized by the location of the tetrahedral hemiacetal oxygen in the oxyanion hole and the formation of hydrogen bonds to the backbone NH groups of Ser195 and Gly193. The first transition state analogs were developed using substrate analogs in which the carbonyl of the scissile amide bond of a peptide was replaced by an aldehyde. The tetrahedral structure has been elucidated by X-ray crystallographic studies. Several other substituents, including trifluoromethyl, difluoromethylene, ester, ketone, and α-ketoheterocycles, are transition state analogs (Lucas et al., 2013).

A number of peptide chloromethyl ketones and α-aminoalkylphosphonate diaryl esters have been designed and tested with PR3 (Kam et al., 1992a; Grzywa and Sieńczyk, 2013). Peptide chloromethyl

TABLE 4
Peptide-based synthetic inhibitors blocking human PR3 activity

Inhibitor	PR3	Elastase	Reference
Covalent inhibitors, $k_{\mathrm{obs/[I]}}$ (M^{-1}s^{-1})			
Peptide chloromethyl ketones			
MeO-Suc-Ala-Ala-Pro-Val-CH$_2$Cl	5.9	1600	Kam et al., 1992a
Bt-AHX-Pro-Tyr-Phe-Ala-CH$_2$Cl	18	N.S.	Guarino et al., unpublished data
Peptide phosphonate esters			
Boc-Val-Pro-Val^P(O-C$_6$H$_5$)$_2$	46	27,000	Kam et al., 1992a
MeO-Suc-Ala-Ala-Pro-Val^P(O-C$_6$H$_5$)$_2$	150	7100	Kam et al., 1992a
MeO-Suc-Ala-Ala-Ala-Val^P(O-C$_6$H$_5$)$_2$	30	1500	Kam et al., 1992a
MeO-Suc-Ala-Ala-Pro-norVal^P(O-C$_6$H$_5$)$_2$	21	380	Kam et al., 1992a
Bt-Val-Pro-Abu^P(O-C$_6$H$_4$-4-S-CH$_3$)$_2$	5100	420,000	Grzywa et al., 2014
Bt-Val-Pro-Val^P(O-C$_6$H$_4$-4-S-CH$_3$)$_2$	16,000	550,000	Grzywa et al., 2014
Bt-Val-Pro-Leu^P(O-C$_6$H$_4$-4-COOCH$_3$)$_2$	19,000	210,000	Grzywa et al., 2014
Bt-[PEG]$_4$-Nle(O-Bzl)-Met(O)$_2$-Oic-Abu^P(O-C$_6$H$_5$)$_2$	93,000	1,4000,000	Kasperkiewicz et al., 2014
Ac-Asp-Tyr-Asp-Ala^P(O-C$_6$H$_4$-4-Cl)$_2$	1.9	N.S.	Guarino et al., 2014
Ac-Pro-Tyr-Asp-Ala^P(O-C$_6$H$_4$-4-Cl)$_2$	154	N.S.	Guarino et al., 2014
Bt-Pro-Tyr-Asp-Ala^P(O-C$_6$H$_4$-4-Cl)$_2$	4168	N.S.	Guarino et al., 2014
HX-Pro-Tyr-Asp-Ala^P(O-C$_6$H$_4$-4-Cl)$_2$	4118	N.S.	Guarino et al., 2014
Ac-AHX-Pro-Tyr-Asp-Ala^P(O-C$_6$H$_4$-4-Cl)$_2$	2159	N.S.	Guarino et al., 2014
Bt-[PEG]$_{66}$-Pro-Tyr-Asp-Ala^P(O-C$_6$H$_4$-4-Cl)$_2$	1163	46	Guarino et al., 2014
Reversible inhibitors, K_i (μM)			
Pseudopeptides			
ABZ-Val-Ala-Asp-(aza)norVal-Ala-Asp-Tyr-Gln-Tyr$_{NO_2}$	1.5	N.S.	Epinette et al., 2012
ABZ-Val-Ala-Asp-norVal[Ψ](COCH$_2$)-Ala-Asp-Tyr-Gln-EDDnp	1.7	N.S.	Budnjo et al., 2014
ABZ-Val-Ala-Asn-norVal[Ψ](COCH$_2$)-Ala-Glu-Arg-Gln-EDDnp	9.1	N.S.	Budnjo et al., 2014

Ac, Acetyl; AHX, 6-amino-hexanoic acid; ABZ, *ortho*-aminobenzoic acid; Boc, *t*-butoxycarbonyl; Bt, biotin; EDDnp, *N*-(2.4-dinitrophenyl) ethylenediamine; HX, hexanoic acid; MeO, methoxy; N.S., not significant.

ketones inhibit serine and cysteine proteases, whereas α-aminoalkylphosphonate diaryl esters selectively inhibit serine proteases. α-Aminoalkylphosphonate diaryl esters do not crossreact with acetylcholinesterase or with threonine, aspartyl, and metalloproteases (Grzywa and Sieńczyk, 2013). They are chemically stable, nontoxic compounds at acidic and neutral buffer conditions and in plasma (but are hydrolyzed rapidly at an alkaline pH above 8). The in vivo activity of α-aminophosphonate derivatives has been evaluated in animal models (Sieńczyk and Oleksyszyn, 2009). Design of these inhibitors has primarily focused on the attachment of the serine trap to the recognition sequence present in a known peptidyl substrate of PR3 (Fig. 8A). These inhibitors interact covalently by the catalytic triad residues and can also be used as activity-based probes (Grzywa and Sieńczyk, 2013). The mechanism of inactivation of peptide chloromethyl ketones involves recognition of the peptide moiety by PR3, nucleophilic action of the Ser195 with the carbonyl of the chloromethyl ketone to give the tetrahedral structure, and alkylation of the nitrogen of the imidazole ring of the active site histidine. MeO-Suc-AAPV-CH$_2$Cl was one the first irreversible PR3 inhibitors identified, with a very low $k_{\mathrm{obs/[I]}}$ of 5.9 M^{-1}s^{-1}. Bt-6-amino hexanoic acid-Pro-Tyr-Phe-Ala-CH$_2$Cl has been identified selective to PR3 over HNE (Table 4).

Several α-aminoalkylphosphonate diaryl ester compounds blocking PR3 and HNE activities are shown in Table 4. We recently designed and synthesized new phosphonate inhibitors based on structural differences between PR3 and HNE (Guarino et al., 2014). The combination of a prolyl residue at P4 and an aspartyl residue at P2 yielded the first selective chlorodiphenyl phosphonate inhibitors of PR3 with the structure Ac-peptidyl^P(O-C$_6$H$_4$-4-Cl)$_2$. These inhibitors are resistant to degradation and can inactivate PR3 in biologic samples. The replacement of the N-terminal acetyl group by hexanoic acid, 6-amino-hexanoic acid, or biotin resulted in a significant improvement in the $k_{\mathrm{obs/[I]}}$ value (Table 4). The N-terminally biotinylated inhibitor containing polyethylene glycol (PEG) as a spacer Bt-[PEG]$_{66}$-Pro-Tyr-Asp-Ala^P(O-C$_6$H$_4$-4-Cl)$_2$ acts as activity-based probe and can be used to visualize cellular or extracellular PR3 in native conditions using labeled extravidin/avidin (Guarino et al., 2014) (Fig. 8B). This compound is a highly useful tool to identify soluble active PR3 in biologic samples, such as inflammatory lung secretions and the urine of patients with bladder cancer. The same compound can also be taken to visualize intracellular PR3 and PR3^m on activated neutrophils (Guarino et al., 2014).

3. Mechanism-Based Inhibitors. Mechanism-based inhibitors, also called suicide inhibitors, are initially unreactive molecules that are processed by the target proteases. This processing results in the unmasking of a reactive function present in the inhibitor. The unmasked groups that are highly reactive electrophilic species can then react with an active site nucleophilic residue to give an irreversibly blocked protease. Most compounds initially react with Ser195 and form an acyl-enzyme complex, while the reactive group is simultaneously
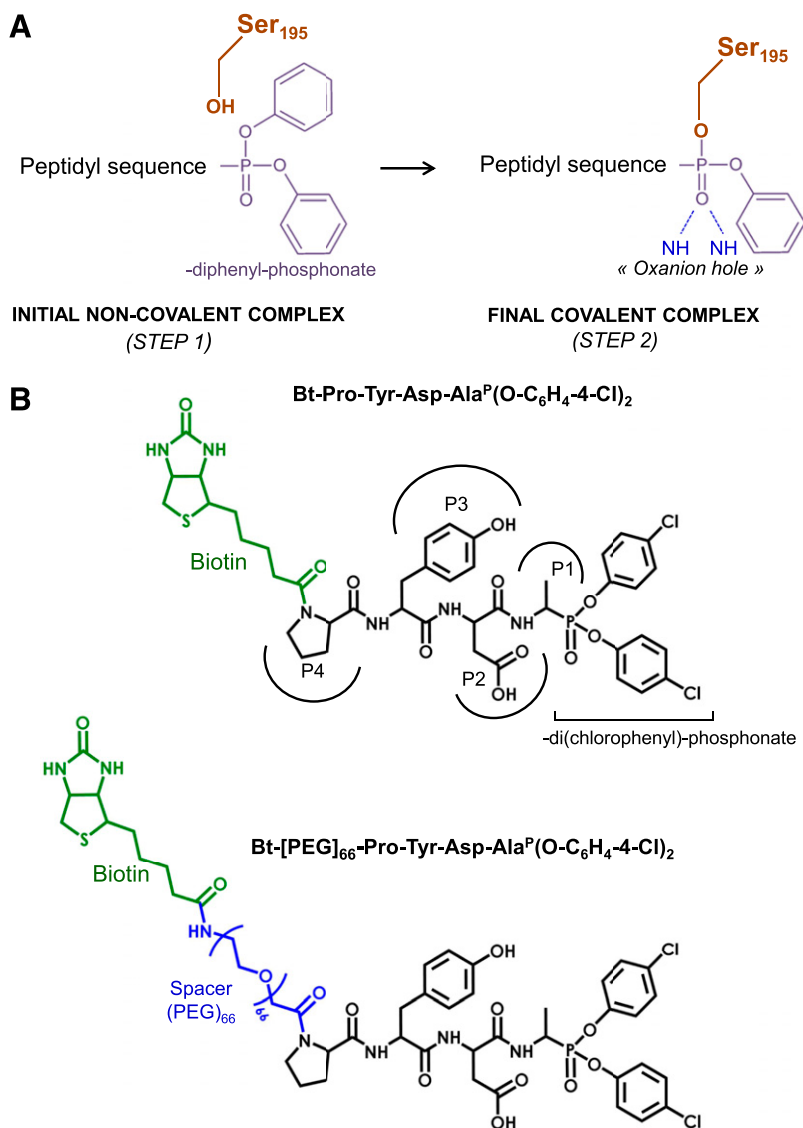
Fig. 8. Chemical structures of selective biotinylated chlorodiphenyl phosphonate inhibitors of PR3. (A) Mechanism of inhibition of serine proteases by diphenyl phosphonate ester. (B) Chemical structures of the biotinylated inhibitors Bt-Pro-Tyr-Asp-Ala^P(O-C$_6$H$_4$-4-Cl)$_2$ and Bt-[PEG]$_{66}$-Pro-Tyr-Asp-Ala^P(O-C$_6$H$_4$-4-Cl$_2$) (Guarino et al., 2014).

unmasked. One advantage of the mechanism-based inhibitors is their good target selectivity due to the presence of a latent electrophilic group, which is unmasked only after protease-induced processing. A variety of templates, including the coumarins, isocoumarins, 2,5-thiadiazolidin-3-one 1, and succinimide, have been used to inhibit serine proteases (Zhong and Groutas, 2004; Lucas et al., 2013).
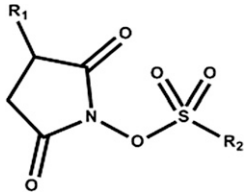
Chloroisocoumarins are heterocyclic compounds that contain masked acid chlorides. These compounds were the first mechanism-based inhibitors to be reported for HNE (Harper and Powers, 1985; Harper et al., 1985). Kam et al. (1992a,b) showed that 3,4-dichloroisocoumarin, a general inhibitor of serine proteases, inhibited PR3 with a $k_{obs/[I]}$ of 2600 M^{-1}s^{-1}. Other substituted isocoumarins such as 7-amino-4-chloro-3-(2-bromoethoxy)isocoumarin can also inhibit PR3 ($k_{obs/[I]}$ = 4700 M^{-1}s^{-1}).

Groutas et al. (1989) synthesized a series of molecules derived from 3-alkyl-N-hydroxy succinimide derivatives and showed their efficiency against HNE. These derivatives have also been shown to be highly effective inhibitors of PR3. The $k_{obs/[I]}$ values of the best compounds are summarized in (summarized in Table 5). Groutas et al. (1998) later developed serine protease inhibitors based on the 1,2,5-thiadiazolidin-3-one 1,1-dioxide scaffold. Sulfone derivatives of the first series of compounds were found to be highly effective for HNE and PR3 (Groutas et al., 1998) (Table 6). The mechanism of action of the 1,2,5-thiadiazolidin-3-one 1,1-dioxide scaffold inhibitors was elucidated by determining the X-ray structure of a compound in complex with HNE (Huang et al., 2008) (Fig. 9A).

4. Alternate Substrate Inhibitors (Acylating Inhibitors). Alternate substrate inhibitors, also called acylating inhibitors, inhibit serine proteases

TABLE 5
N-hydroxysuccinimide derivative inhibitors blocking human PR3 activity

		$k_{obs/[I]}$	
		PR3	Elastase
		$M^{-1}s^{-1}$	
R_1	R_2		
n-Propyl	Methyl	8600[a]	8600[b]
Isopropyl	trans-Styryl	8100[a]	100,000[b]
Isobutyl	trans-Styryl	10,400[a]	N.D.[c]

[a]Values from Groutas et al. (1990).
[b]Values from Groutas et al. (1989).
[c]Inactivation was too fast to measure by sampling techniques (Groutas et al., 1989).

TABLE 6
1,2,5-thiadiazolidin-3-one 1,dioxide derivatives blocking human PR3 activity

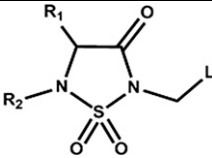| | | | $k_{obs/[I]}$ | |
			PR3	Elastase
			$M^{-1}s^{-1}$	
R_1	R_2	L		
Isobutyl	(m-COOCH$_3$)Bzl	SO$_2$Ph	7080	63,600
Isobutyl	(m-COCH)Bzl	SO$_2$Ph	10,300	38,700
Isobutyl	Benzyl	SO$_2$(p-Cl phenyl)	16,200	219,000
Isobutyl	Benzyl	SO$_2$CH$_2$(p-Cl phenyl)	20,300	165,000

Values are from Groutas et al. (1998).

by acetylating the active site serine residue. The mechanism of this process involves the displacement of a leaving group from the acylating agent. Heterocylic structures including β-lactams, cephalosphorine sulphones, and benzoxazin-4-ones (Teshima et al., 1982; Hedstrom et al., 1984) give extremely stable enzyme-inhibitor complexes that undergo very slow deacylation (Zhong and Groutas, 2004; Lucas et al., 2013).

A cephalosporin derivative developed by Merck, L-658,758 [1-[[3-(acetoxymethyl)-7α-methoxy-8-oxo-5-thia-1-azabicyclo[4.2.01]oct-2-en-2-yl]carbonyl] proline S,S-dioxide], was initially identified as a potent inhibitor of HNE ($k_{obs/[I]}$ = 3800 $M^{-1}s^{-1}$) (Doherty et al., 1986; Finke et al., 1992). Rees et al. (1997) demonstrated that L-658,758 was also an efficient inhibitor of PR3. The mechanism for the inhibition by cephalosporins involves the initial formation of a Michaelis complex followed by acylation of the active site serine. The group on the 3'-methylene is released during the course of these reactions. A stable HNE inhibitor complex arises from the addition on the active site His to the 3'-methylene. L-658,758 is a functionally irreversible HNE inhibitor with a 9-hour half-life (Knight et al., 1992). Its efficacy has been shown in a hamster lung hemorrhage model (Finke et al., 1992).

Sivelestat sodium hydrate (N-[2-[4-(2,2-dimethyl-propionyloxy)-phenylsulfonyl-amino]benzoyl] aminoacetic acid; research name ONO-5046, marketed as Elaspol; Ono Pharmaceutical Co., Ltd, Osaka, Japan) was developed as a potent and intravenously effective HNE inhibitor, with an IC$_{50}$ of 0.044 μM and a K_i of 0.2 μM (Kawabata et al., 1991). Sivelestat is approved in Japan and Korea and is clinically used to treat acute respiratory distress syndrome (Aikawa and Kawasaki, 2014). Sivelestat can also inhibit PR3, with an IC$_{50}$ of 0.034 μM (Hwang et al., 2015). A 2-aminobenzaldehyde oxime analog of sivelestat was recently synthesized (Fig. 9B) and was found to be slightly more potent against PR3 than sivelestat, with an IC$_{50}$ of 0.022 μM

(Hwang et al., 2015). The efficacy of the latter compound was recently demonstrated in an lipopolysaccharide-induced paw edema model in mice (Hwang et al., 2015).

V. Proteinase 3–Targeting Inhibitors and Antibodies as Therapeutic Tools

NSPs stored in primary granules are tightly contained by natural inhibitors both in the extracellular microenvironment and in the cytosol of neutrophils and their precursors. Deficiencies in the performance of inhibitors are mostly associated with sustained inflammation and enhanced neutrophil-mediated tissue injury. The role of a cytoplasmic serpin, serpinB1, targeting NE, CatG, and PR3 has been extensively studied in experimental models with mice completely lacking serpinB1. Local release of serpinB1 from dying neutrophils and intracellular neutralization of NSP activities across leaky granule membranes reduces collateral tissue injury and improves lung defense responses and pathogen clearance by neutrophils (Benarafa et al., 2007).

In the absence of the NSP inhibitor serpinB1, surfactant protein D was strongly degraded and host defense against Pseudomonas infections of the lungs was impaired, resulting in increased mortality of serpinB1-deficient mice compared with wild-type mice (Stolley et al., 2012). SerpinB1 has also been detected in the bronchoalveolar lavage fluid of patients with cystic fibrosis and is known to inhibit HNE (Cooley et al., 2011), CatG, and PR3 (Gong et al., 2011). Its anti-inflammatory effect on the immune response to lung infections is also mediated by reducing the formation of neutrophil extracellular traps (Farley et al., 2012).

PR3 can accelerate spontaneous apoptotic cell death of neutrophils by cleaving procaspase-3 (Pederzoli et al., 2005) and may determine the lifespan and survival of neutrophils during inflammation. Although cytoplasmic proteins are not accessible to PR3 located in the lumen of granules, leakiness and permeability of granule membranes increases with the aging of neutrophils. In parallel, the cytosolic content of inhibitors declines and paves the way for elastolytic activities in the cytosol and
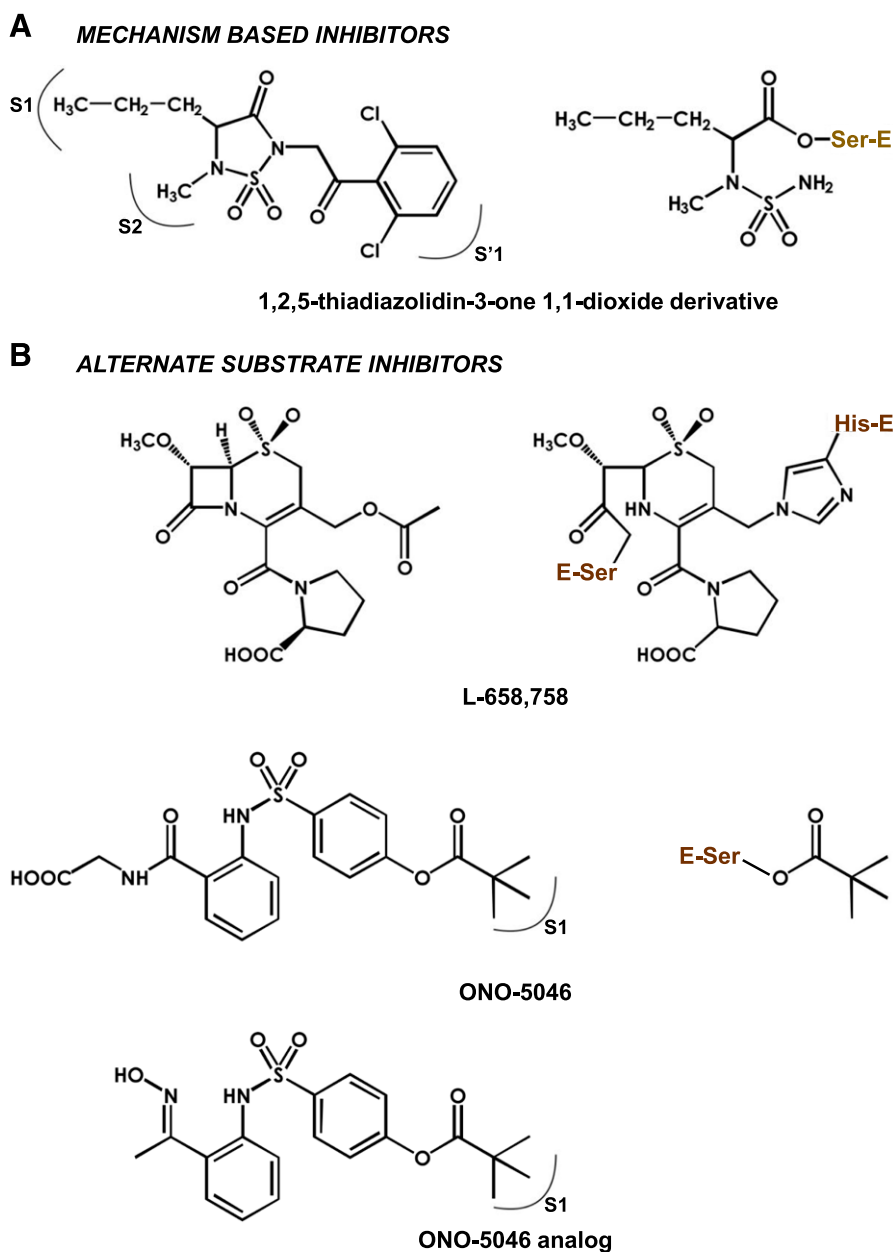
Fig. 9. Mechanism-based and alternate substrate inhibitors of PR3. (A) Chemical structure of mechanism-based inhibitor of PR3 1,2,5-thiadiazolidin-3-one 1, the dioxide derivative (R1 = *n*-propyl; R2 = methyl; L2 = 2,6-dichlorobenzoate) (left), and its postulated mechanism of action elucidated by the X-ray crystal structure (Huang et al., 2008) (right). (B) Chemical structures of alternate substrate inhibitors of PR3 L-658.758, ONO-5046, an ONO-5046 analog, and their postulated mechanism of action.

nucleus of neutrophils. Concomitant with these age-related changes, PR3-deficient mice (Loison et al., 2014) display a delay in neutrophil cell death and a stronger accumulation of neutrophils at sites of inflammation.

An altered balance between the cytosolic inhibitor serpinB1 and PR3 may improve the capabilities of neutrophils to combat infections in peripheral tissues but could also augment tissue damage. Likewise, cleavage of annexin 1 by PR3 in the context of neutrophil activation reduces the anti-inflammatory activity of annexin 1 and points to a proinflammatory role of PR3. Transfer of PR3 into the cytosol of endothelial cells during neutrophil–endothelial cell interactions has also

been inferred as a trigger of endothelial cell apoptosis, which appears to contribute to small vessel damage at sites of inflammation (Pendergraft et al., 2004; Jerke et al., 2015).

Although recombinant production of serpinB1 has been achieved at a larger scale (Cooley et al., 1998), it is still questionable whether externally added serpinB1 is therapeutically effective and significantly outperforms the endogenous anti-inflammatory action of the cytosolic homolog. A serpinB1 mutant that strongly and specifically inhibits PR3 was recently developed (Jégot et al., 2011). Such a fast-acting inhibitor could serve as a supplemental therapy administered by vascular or

aerosol routes, provided that it is resistant enough against inactivation by proteases and oxidation by oxygen radicals of the extracellular environment.

α1PI, a natural plasma inhibitor of HNE and PR3, has been extensively evaluated in various clinical settings. α1PI is the main inhibitor of HNE and PR3 in the lower respiratory tract but it shows a strong preference for HNE over PR3 in case of a simultaneous presence of the two proteases (Korkmaz et al., 2005b). Although other locally acting elastase inhibitors (e.g., secretory leukocyte SLPI and elafin) provide some protection against NE and PR3 in humans, only decreased levels of plasma α1PI are known to be associated with chronic diseases. Gene mutations in α1PI with reduced inhibitory plasma levels frequently cause emphysema and COPD, more rarely cause liver disease (Duvoix et al., 2014), and occasionally cause a skin disease presenting as necrotizing panniculitis (Vigl et al., 2015). α1PI dysfunction has also been associated with an increased risk of ANCA-associated vasculitis (Mahr et al., 2010).

According to a recent genome-wide association study, most of the reduced α1PI levels in plasma are explained by specific germline mutations leading to the S and Z variants but do not accurately predict the degree of deterioration of long-term lung function (Thun et al. 2013). Other factors, such as inflammatory mediators and the tissue-specific regulation of α1PI, may play a role in lung disease among individuals with α1PI deficiency. Environmental factors that induce neutrophil recruitment and inflammation in the lungs, particularly smoking but also occupational dust exposure, allergens, and infective agents, are important cofactors that accelerate the development of emphysema in patients with α1PI deficiency (Cavarra et al., 2001; Abusriwil and Stockley, 2006; Gooptu and Lomas, 2009; Brebner and Stockley, 2013). Under these pathophysiological conditions, levels of functional α1PI decline in tissues as a consequence of local inactivation through proteases, oxidation, or degradation. Specific inactivation of plasma α1PI within the RCL was identified in patients with sepsis (Kiehntopf et al., 2011). With regard to PR3 inhibition, the association rate constants for the Z and M variants of α1PI are very similar but are 15-fold lower compared with NE. This relative inefficiency of PR3 inhibition by α1PI variants implies that PR3 activity persists for a longer time period than NE activity under conditions of reduced local α1PI tissue availability. Thus, NE is preferentially inhibited by M-α1PI and Z-α1PI, and PR3 escapes inhibition when local tissue concentrations are low. Alternatively, synthetic or antibody-based inhibitors that specifically target the PR3 active site can be developed.

Millet et al. (2015) recently demonstrated that proteolytically active PR3 on the membrane of apoptotic cells promotes sustained inflammation, thus providing additional support for the development of novel therapeutic strategies aiming to inhibit PR3 activity at the surface of immune cells. However, PR3^m on the outer surface of activated neutrophils is hardly inhibited by endogenous and small synthetic inhibitors. This is attributable to the resting-state conformation of induced PR3^m that impairs the productive binding of substrates and inhibitors and to the previous observation that constitutive PR3^m is proteolytically inactive (Guarino et al., 2014). α1PI, however, dissociates induced PR3^m from the surface of activated neutrophils, forming irreversible and proteolytically inactive complexes, but it cannot prevent the binding of C-ANCAs to constitutive PR3 and subsequent activation of neutrophils (Guarino et al., in preparation). An alternative to prevent neutrophil activation by C-ANCAs would be to use anti-PR3 mAb fragments without the Fc domain that masks the major epitope recognized by C-ANCAs on both constitutive and induced PR3. However, an ideal solution would be to target both the protease active site and a major epitope at the protease surface through allosteric inhibition by exosite-targeting mAbs, as was successfully reported for membrane-bound matriptase-1 (Ganesan et al., 2010). For this purpose, single domain antibodies from camelids, so-called nanobodies, offer a large advantage over mammalian two-chain Fab antibody fragments, including high solubility, high thermal stability, and good tissue penetration. They possess antigen-binding CDR3 loops that can extend into the active site cleft of enzymes and can directly interfere with catalytic functions (Wesolowski et al., 2009). Such antibodies are promising therapeutic tools to block neutrophil-activating C-ANCA binding and the proinflammatory function of pathogenic PR3^m on apoptotic neutrophils.

VI. Indirect Targeting of Proteinase 3 in Diseases

Instead of directly targeting mature PR3 and other NSPs, novel approaches to decrease the whole-body pool of NSPs have been developed and evaluated in preclinical models (Méthot et al., 2008). Before active NSPs are stored in cytoplasmic granules of neutrophils, they are biosynthetically processed by CatC (see section II).

CatC is a papain-like cysteine protease that removes dipeptides from the N-terminal end of a variety of proteins (Turk et al., 2001). The best characterized substrates of CatC are the proforms of NSPs in promyelocytic precursor cells of the bone marrow (McGuire et al., 1993; Adkison et al., 2002). CatC itself is synthesized as a proprotein and then processed through proteolytic cleavage to release an N-terminal exclusion domain, an activation peptide (propeptide), a heavy chain, and a light chain (Dahl et al., 2001). The protease involved in these physiologic cleavages has not yet been identified (Mallen-St Clair et al., 2006). Inactivation of CatC as seen in patients with the Papillon-Lefèvre syndrome and in knockout mice dramatically lowers the

storage pool of active serine proteases in mature neutrophils by an as-yet-unknown mechanism (Adkison et al., 2002; Pham et al., 2004; Sørensen et al., 2014). Because the clinical consequences of inborn CatC deficiency are mild, it has been assumed that small-molecule inhibitors of CatC are relatively safe drugs that reduce the neutrophil-associated protease burden in various patients. Small-molecule inhibitors of CatC were indeed shown to reduce serine protease activities of neutrophils (including the autoantigen of patients with GPA, PR3) from circulating neutrophils (Méthot et al., 2007, 2008). High fractional inhibition of CatC is a prerequisite to reach therapeutically significant effects (Méthot et al., 2007, 2008). This requires large amounts of inhibitors, a condition that is hardly met with an in vivo use. Controlling the activity of CatC may be achieved by either using small synthetic inhibitors or impairing the maturation of its proform into an active protease. Pro-CatC maturation is mainly controlled by cysteine proteases, with cathepsin S (CatS) being a major actor in human neutrophil precursors cells (Hamon et al., 2016). Several CatS inhibitors were recently developed and are currently in clinical trials (Wilkinson et al., 2015). The combination of CatS and CatC inhibitors should not only reduce the NSP burden within neutrophils, but it should also impair cell recruitment at inflammatory sites. Hence, we anticipate that inhibition of CatC in the precursor cells of the bone marrow represents an attractive therapeutic strategy resulting in better protection against neutrophil-mediated tissue damage than local administration of combinations of selective small-molecule inhibitors against each NSP, especially in individuals with α1PI deficiency and in patients with GPA (Guay et al., 2010; Korkmaz et al., 2013b).

VII. Conclusions and Future Directions

Because of its close structural and functional resemblance with HNE, PR3 has long been considered as a redundant protease of minor interest. The discovery that the autoimmune response exclusively to PR3, and not to HNE, is a central pathogenic feature of GPA has been the first evidence for its distinct pathophysiological properties. Since then, a variety of specific biochemical functions have been reported. Most of these functions are related to PR3's unique spatiotemporal pattern of expression that differs from the other NSPs, especially from HNE. Although PR3 is initially stored only in the same granular fraction (like HNE), its constitutive and inducible expression on the surface of circulating neutrophils makes it the prime target of autoantibodies in a clearly distinct autoimmune syndrome. PR3^m is hardly inhibited by chemical and endogenous inhibitors at the cell surface of neutrophils, as opposed to other NSPs. The demonstration of PR3 recapture and internalization by endothelial cells has increased its panel of functions by providing evidence for a role in triggering cellular responses during vascular inflammation.

The in-depth investigation of PR3's substrate specificity also provided evidence for its role as a specific protein-degrading enzyme. Interestingly, there is currently no endogenous protease inhibitor that preferentially targets PR3 so it may remain quantitatively the principal active NSP in a biologic environment initially overwhelmed by HNE and other NSPs. Controlling PR3 activity efficiently is a timely and important issue, the effects of which have only been partially addressed up to now. Indeed, different approaches must be explored to suppress the activity of intracellular PR3, PR3^m, or secreted PR3 either as a free protease or trapped within the extracellular matrix of various organs.

The large repertoire of tools that are currently in development should allow efficient targeting of PR3 no matter the pathophysiological context. An upstream control may be achieved by targeting the maturation of proteases that activate its proform, whereas a downstream control may result from the use of competing antibodies that impair the access of substrates to the active site or by cell-permeable synthetic inhibitors and recombinant proteins that completely occlude the active site region of PR3.

References

Abusriwil H and Stockley RA (2006) Alpha-1-antitrypsin replacement therapy: current status. *Curr Opin Pulm Med* **12**:125–131.

Adessi C and Soto C (2002) Converting a peptide into a drug: strategies to improve stability and bioavailability. *Curr Med Chem* **9**:963–978.

Adkison AM, Raptis SZ, Kelley DG, and Pham CT (2002) Dipeptidyl peptidase I activates neutrophil-derived serine proteases and regulates the development of acute experimental arthritis. *J Clin Invest* **109**:363–371.

Aikawa N and Kawasaki Y (2014) Clinical utility of the neutrophil elastase inhibitor sivelestat for the treatment of acute respiratory distress syndrome. *Ther Clin Risk Manag* **10**:621–629.

Baggiolini M, Bretz U, Dewald B, and Feigenson ME (1978) The polymorphonuclear leukocyte. *Agents Actions* **8**:3–10.

Baggiolini M, Schnyder J, Bretz U, Dewald B, and Ruch W (1979) Cellular mechanisms of proteinase release from inflammatory cells and the degradation of extracellular proteins. *Ciba Found Symp* **75**:105–121.

Barrett AJ and Starkey PM (1973) The interaction of alpha 2-macroglobulin with proteinases. Characteristics and specificity of the reaction, and a hypothesis concerning its molecular mechanism. *Biochem J* **133**:709–724.

Beatty K, Bieth J, and Travis J (1980) Kinetics of association of serine proteinases with native and oxidized alpha-1-proteinase inhibitor and alpha-1-antichymotrypsin. *J Biol Chem* **255**:3931–3934.

Benarafa C, Priebe GP, and Remold-O'Donnell E (2007) The neutrophil serine protease inhibitor serpinb1 preserves lung defense functions in Pseudomonas aeruginosa infection. *J Exp Med* **204**:1901–1909.

Benarafa C and Remold-O'Donnell E (2005) The ovalbumin serpins revisited: perspective from the chicken genome of clade B serpin evolution in vertebrates. *Proc Natl Acad Sci USA* **102**:11367–11372.

Bode W, Wei AZ, Huber R, Meyer E, Travis J, and Neumann S (1986) X-ray crystal structure of the complex of human leukocyte elastase (PMN elastase) and the third domain of the turkey ovomucoid inhibitor. *EMBO J* **5**:2453–2458.

Bories D, Raynal MC, Solomon DH, Darzynkiewicz Z, and Cayre YE (1989) Down-regulation of a serine protease, myeloblastin, causes growth arrest and differentiation of promyelocytic leukemia cells. *Cell* **59**:959–968.

Borregaard N (2010) Neutrophils, from marrow to microbes. *Immunity* **33**:657–670.

Brebner JA and Stockley RA (2013) Recent advances in α-1-antitrypsin deficiency-related lung disease. *Expert Rev Respir Med* **7**:213–229, quiz 230.

Budnjo A, Narawane S, Grauffel C, Schillinger AS, Fossen T, Reuter N, and Haug BE (2014) Reversible ketomethylene-based inhibitors of human neutrophil proteinase 3. *J Med Chem* **57**:9396–9408.

Campanelli D, Melchior M, Fu Y, Nakata M, Shuman H, Nathan C, and Gabay JE (1990) Cloning of cDNA for proteinase 3: a serine protease, antibiotic, and auto-antigen from human neutrophils. *J Exp Med* **172**:1709–1715.

Campbell EJ, Campbell MA, and Owen CA (2000) Bioactive proteinase 3 on the cell surface of human neutrophils: quantification, catalytic activity, and susceptibility to inhibition. *J Immunol* **165**:3366–3374.

Capizzi SA, Viss MA, Hummel AM, Fass DN, and Specks U (2003) Effects of carboxy-terminal modifications of proteinase 3 (PR3) on the recognition by PR3-ANCA. *Kidney Int* **63**:756–760.

Cavarra E, Lucattelli M, Gambelli F, Bartalesi B, Fineschi S, Szarka A, Giannerini F, Martorana PA, and Lungarella G (2001) Human SLPI inactivation after cigarette smoke exposure in a new in vivo model of pulmonary oxidative stress. *Am J Physiol Lung Cell Mol Physiol* **281**:L412–L417.

Cooley J, Mathieu B, Remold-O'Donnell E, and Mandle RJ (1998) Production of recombinant human monocyte/neutrophil elastase inhibitor (rM/NEI). *Protein Expr Purif* **14**:38–44.

Cooley J, Sontag MK, Accurso FJ, and Remold-O'Donnell E (2011) SerpinB1 in CF airway fluids: quantity, molecular form and mechanism of elastase inhibition. *Eur Respir J* **37**:1083–1090.

Cooley J, Takayama TK, Shapiro SD, Schechter NM, and Remold-O'Donnell E (2001) The serpin MNEI inhibits elastase-like and chymotrypsin-like serine proteases through efficient reactions at two active sites. *Biochemistry* **40**:15762–15770.

Courtney M, Jallat S, Tessier LH, Benavente A, Crystal RG, and Lecocq JP (1985) Synthesis in E. coli of alpha 1-antitrypsin variants of therapeutic potential for emphysema and thrombosis. *Nature* **313**:149–151.

Crystal RG, Brantly ML, Hubbard RC, Curiel DT, States DJ, and Holmes MD (1989) The alpha 1-antitrypsin gene and its mutations. Clinical consequences and strategies for therapy. *Chest* **95**:196–208.

Csernok E, Lüdemann J, Gross WL, and Bainton DF (1990) Ultrastructural localization of proteinase 3, the target antigen of anti-cytoplasmic antibodies circulating in Wegener's granulomatosis. *Am J Pathol* **137**:1113–1120.

Dahl SW, Halkier T, Lauritzen C, Dolenc I, Pedersen J, Turk V, and Turk B (2001) Human recombinant pro-dipeptidyl peptidase I (cathepsin C) can be activated by cathepsins L and S but not by autocatalytic processing. *Biochemistry* **40**:1671–1678.

David A, Fridlich R, and Aviram I (2005) The presence of membrane Proteinase 3 in neutrophil lipid rafts and its colocalization with FcγRIIIb and cytochrome b558. *Exp Cell Res* **308**:156–65.

Dementiev A, Dobó J, and Gettins PG (2006) Active site distortion is sufficient for proteinase inhibition by serpins: structure of the covalent complex of alpha1-proteinase inhibitor with porcine pancreatic elastase. *J Biol Chem* **281**:3452–3457.

Dementiev A, Simonovic M, Volz K, and Gettins PG (2003) Canonical inhibitor-like interactions explain reactivity of alpha1-proteinase inhibitor Pittsburgh and antithrombin with proteinases. *J Biol Chem* **278**:37881–37887.

Doan N and Gettins PG (2007) Human alpha2-macroglobulin is composed of multiple domains, as predicted by homology with complement component C3. *Biochem J* **407**:23–30.

Doherty JB, Ashe BM, Argenbright LW, Barker PL, Bonney RJ, Chandler GO, Dahlgren ME, Dorn CP Jr, Finke PE, and Firestone RA, et al. (1986) Cephalosporin antibiotics can be modified to inhibit human leukocyte elastase. *Nature* **322**:192–194.

Dolman KM, van de Wiel BA, Kam CM, Kerrigan JE, Hack CE, von dem Borne AE, Powers JC, and Goldschmeding R (1993) Proteinase 3: substrate specificity and possible pathogenetic effect of Wegener's granulomatosis autoantibodies (c-ANCA) by dysregulation of the enzyme. *Adv Exp Med Biol* **336**:55–60.

Dorn CP, Zimmerman M, Yang SS, Yurewicz EC, Ashe BM, Frankshun R, and Jones H (1977) Proteinase inhibitors. I. Inhibitors of elastase. *J Med Chem* **20**:1464–1468.

Duvoix A, Roussel BD, and Lomas DA (2014) Molecular pathogenesis of alpha-1-antitrypsin deficiency. *Rev Mal Respir* **31**:992–1002.

Elliott PR, Lomas DA, Carrell RW, and Abrahams JP (1996) Inhibitory conformation of the reactive loop of alpha 1-antitrypsin. *Nat Struct Biol* **3**:676–681.

Epinette C, Croix C, Jaquillard L, Marchand-Adam S, Kellenberger C, Lalmanach G, Cadene M, Viaud-Massuard MC, Gauthier F, and Korkmaz B (2012) A selective reversible azapeptide inhibitor of human neutrophil proteinase 3 derived from a high affinity FRET substrate. *Biochem Pharmacol* **83**:788–796.

Farley K, Stolley JM, Zhao P, Cooley J, and Remold-O'Donnell E (2012) A serpinB1 regulatory mechanism is essential for restricting neutrophil extracellular trap generation. *J Immunol* **189**:4574–4581.

Finke PE, Shah SK, Ashe BM, Ball RG, Blacklock TJ, Bonney RJ, Brause KA, Chandler GO, Cotton M, and Davies P, et al. (1992) Inhibition of human leukocyte elastase. 4. Selection of a substituted cephalosporin (L-658,758) as a topical aerosol. *J Med Chem* **35**:3731–3744.

Fujinaga M, Chernaia MM, Halenbeck R, Koths K, and James MN (1996) The crystal structure of PR3, a neutrophil serine proteinase antigen of Wegener's granulomatosis inhibitors. *J Mol Biol* **261**:267–278.

Gabillet J, Millet A, Pederzoli-Ribeil M, Tacnet-Delorme P, Guillevin L, Mouthon L, Frachet P, and Witko-Sarsat V (2012) Proteinase 3, the autoantigen in granulomatosis with polyangiitis, associates with calreticulin on apoptotic neutrophils, impairs macrophage phagocytosis, and promotes inflammation. *J Immunol* **189**:2574–2583.

Ganesan R, Eigenbrot C, and Kirchhofer D (2010) Structural and mechanistic insight into how antibodies inhibit serine proteases. *Biochem J* **430**:179–189.

Garcia-Ferrer I, Arête P, Gómez-Blanco J, Luque D, Duquerroy S, Castón JR, Goulas T, and Gomis-Rüth FX (2015) Structural and functional insights into Escherichia coli α2-macroglobulin endopeptidase snap-trap inhibition. *Proc Natl Acad Sci USA* **112**:8290–8295.

Garwicz D, Lindmark A, Hellmark T, Gladh M, Jögi J, and Gullberg U (1997) Characterization of the processing and granular targeting of human proteinase 3 after transfection to the rat RBL or the murine 32D leukemic cell lines. *J Leukoc Biol* **61**:113–123.

Gauthier F, Fryksmark U, Ohlsson K, and Bieth JG (1982) Kinetics of the inhibition of leukocyte elastase by the bronchial inhibitor. *Biochim Biophys Acta* **700**:178–183.

Gettins PG (2002) Serpin structure, mechanism, and function. *Chem Rev* **102**:4751–4804.

Gong D, Farley K, White M, Hartshorn KL, Benarafa C, and Remold-O'Donnell E (2011) Critical role of serpinB1 in regulating inflammatory responses in pulmonary influenza infection. *J Infect Dis* **204**:592–600.

Gooptu B and Lomas DA (2009) Conformational pathology of the serpins: themes, variations, and therapeutic strategies. *Annu Rev Biochem* **78**:147–176.

Groutas WC, Brubaker MJ, Stanga MA, Castrisos JC, Crowley JP, and Schatz EJ (1989) Inhibition of human leukocyte elastase by derivatives of N-hydroxysuccinimide. A structure-activity-relationship study. *J Med Chem* **32**:1607–1611.

Groutas WC, Hoidal JR, Brubaker MJ, Stanga MA, Venkataraman R, Gray BH, and Rao NV (1990) Inhibitors of human leukocyte proteinase-3. *J Med Chem* **33**:1085–1087.

Groutas WC, Kuang R, Ruan S, Epp JB, Venkataraman R, and Truong TM (1998) Potent and specific inhibition of human leukocyte elastase, cathepsin G and proteinase 3 by sulfone derivatives employing the 1,2,5-thiadiazolidin-3-one 1,1 dioxide scaffold. *Bioorg Med Chem* **6**:661–671.

Groutas WC, Ruan S, Kuang R, Hook JB, and Sands H (1997) Inhibition of human leukocyte proteinase 3 by a novel recombinant serine proteinase inhibitor (LEX032). *Biochem Biophys Res Commun* **233**:697–699.

Grütter MG, Fendrich G, Huber R, and Bode W (1988) The 2.5 A X-ray crystal structure of the acid-stable proteinase inhibitor from human mucous secretions analysed in its complex with bovine alpha-chymotrypsin. *EMBO J* **7**:345–351.

Grzywa R, Burchacka E, Łęcka M, Winiarski Ł, Walczak M, Łupicka-Słowik A, Wysocka M, Burster T, Bobrek K, and Csencsits-Smith K, et al. (2014) Synthesis of novel phosphonic-type activity-based probes for neutrophil serine proteases and their application in spleen lysates of different organisms. *ChemBioChem* **15**:2605–2612.

Grzywa R and Sieńczyk M (2013) Phosphonic esters and their application of protease control. *Curr Pharm Des* **19**:1154–1178.

Guarino C, Legowska M, Epinette C, Kellenberger C, Dallet-Choisy S, Sieńczyk M, Gabant G, Cadene M, Zoidakis J, and Vlahou A, et al. (2014) New selective peptidyl di(chlorophenyl) phosphonate esters for visualizing and blocking neutrophil proteinase 3 in human diseases. *J Biol Chem* **289**:31777–31791.

Guay D, Beaulieu C, and Percival MD (2010) Therapeutic utility and medicinal chemistry of cathepsin C inhibitors. *Curr Top Med Chem* **10**:708–716.

Guyot N, Wartelle J, Malleret L, Todorov AA, Devouassoux G, Pacheco Y, Jenne DE, and Belaaouaj A (2014) Unopposed cathepsin G, neutrophil elastase, and proteinase 3 cause severe lung damage and emphysema. *Am J Pathol* **184**:2197–2210.

Guyot N, Zani ML, Berger P, Dallet-Choisy S, and Moreau T (2005) Proteolytic susceptibility of the serine protease inhibitor trappin-2 (pre-elafin): evidence for tryptase-mediated generation of elafin. *Biol Chem* **386**:391–399.

Hajjar E, Broemstrup T, Kantari C, Witko-Sarsat V, and Reuter N (2010) Structures of human proteinase 3 and neutrophil elastase–so similar yet so different. *FEBS J* **277**:2238–2254.

Hajjar E, Korkmaz B, Gauthier F, Brandsdal BO, Witko-Sarsat V, and Reuter N (2006) Inspection of the binding sites of proteinase3 for the design of a highly specific substrate. *J Med Chem* **49**:1248–1260.

Halbwachs-Mecarelli L, Bessou G, Lesavre P, Lopez S, and Witko-Sarsat V (1995) Bimodal distribution of proteinase 3 (PR3) surface expression reflects a constitutive heterogeneity in the polymorphonuclear neutrophil pool. *FEBS Lett* **374**:29–33.

Hamon Y, Legowska M, Hervé V, Dallet-Choisy S, Marchand-Adam S, Vanderlynden L, Demonte M, Williams R, Scott CJ, and Si-Tahar M, et al. (2016) Neutrophilic cathepsin C is maturated by a multi-step proteolytic process and secreted by activated cells during inflammatory lung diseases. *J Biol Chem* DOI: [published ahead of print].

Hansen G, Gielen-Haertwig H, Reinemer P, Schomburg D, Harrenga A, and Niefind K (2011) Unexpected active-site flexibility in the structure of human neutrophil elastase in complex with a new dihydropyrimidone inhibitor. *J Mol Biol* **409**:681–691.

Harper JW, Hemmi K, and Powers JC (1985) Reaction of serine proteases with substituted isocoumarins: discovery of 3,4-dichloroisocoumarin, a new general mechanism based serine protease inhibitor. *Biochemistry* **24**:1831–1841.

Harper JW and Powers JC (1985) Reaction of serine proteases with substituted 3-alkoxy-4-chloroisocoumarins and 3-alkoxy-7-amino-4-chloroisocoumarins: new reactive mechanism-based inhibitors. *Biochemistry* **24**:7200–7213.

Hedstrom L (2002) Serine protease mechanism and specificity. *Chem Rev* **102**:4501–4524.

Hedstrom L, Moorman AR, Dobbs J, and Abeles RH (1984) Suicide inactivation of chymotrypsin by benzoxazinones. *Biochemistry* **23**:1753–1759.

Hinkofer LC, Hummel AM, Stone JH, Hoffman GS, Merkel PA, Spiera ER, St Clair W, McCune JW, Davis JC, and Specks U, et al. (2015) Allosteric modulation of proteinase 3 activity by anti-neutrophil cytoplasmic antibodies in granulomatosis with polyangiitis. *J Autoimmun* **59**:43–52.

Hinkofer LC, Seidel SA, Korkmaz B, Silva F, Hummel AM, Braun D, Jenne DE, and Specks U (2013) A monoclonal antibody (MCPR3-7) interfering with the activity of proteinase 3 by an allosteric mechanism. *J Biol Chem* **288**:26635–26648.

Hochstrasser K, Reichert R, Schwarz S, and Werle E (1972) [Isolation and characterisation of a protease inhibitor from human bronchial secretion]. *Hoppe Seylers Z Physiol Chem* **353**:221–226.

Hu N, Westra J, and Kallenberg CG (2009) Membrane-bound proteinase 3 and its receptors: relevance for the pathogenesis of Wegener's Granulomatosis. *Autoimmun Rev* **8**:510–514.

Huang W, Yamamoto Y, Li Y, Dou D, Alliston KR, Hanzlik RP, Williams TD, and Groutas WC (2008) X-ray snapshot of the mechanism of inactivation of human

neutrophil elastase by 1,2,5-thiadiazolidin-3-one 1,1-dioxide derivatives. *J Med Chem* **51**:2003–2008.

Hunt LT and Dayhoff MO (1980) A surprising new protein superfamily containing ovalbumin, antithrombin-III, and alpha 1-proteinase inhibitor. *Biochem Biophys Res Commun* **95**:864–871.

Huntington JA, Read RJ, and Carrell RW (2000) Structure of a serpin-protease complex shows inhibition by deformation. *Nature* **407**:923–926.

Hwang TL, Wang WH, Wang TY, Yu HP, and Hsieh PW (2015) Synthesis and pharmacological characterization of 2-aminobenzaldehyde oxime analogs as dual inhibitors of neutrophil elastase and proteinase 3. *Bioorg Med Chem* **23**:1123–1134.

Irving JA, Pike RN, Lesk AM, and Whisstock JC (2000) Phylogeny of the serpin superfamily: implications of patterns of amino acid conservation for structure and function. *Genome Res* **10**:1845–1864.

Jallat S, Carvallo D, Tessier LH, Roecklin D, Roitsch C, Ogushi F, Crystal RG, and Courtney M (1986) Altered specificities of genetically engineered alpha 1 antitrypsin variants. *Protein Eng* **1**:29–35.

Janciauskiene S (2001) Conformational properties of serine proteinase inhibitors (serpins) confer multiple pathophysiological roles. *Biochim Biophys Acta* **1535**:221–235.

Janoff A and Scherer J (1968) Mediators of inflammation in leukocyte lysosomes. IX. Elastinolytic activity in granules of human polymorphonuclear leukocytes. *J Exp Med* **128**:1137–1155.

Jégot G, Derache C, Castella S, Lahouassa H, Pitois E, Jourdan ML, Remold-O'Donnell E, Kellenberger C, Gauthier F, and Korkmaz B (2011) A substrate-based approach to convert SerpinB1 into a specific inhibitor of proteinase 3, the Wegener's granulomatosis autoantigen. *FASEB J* **25**:3019–3031.

Jenne DE, Fröhlich L, Hummel AM, and Specks U (1997) Cloning and functional expression of the murine homologue of proteinase 3: implications for the design of murine models of vasculitis. *FEBS Lett* **408**:187–190.

Jenne DE and Kuhl A (2006) Production and applications of recombinant proteinase 3, Wegener's autoantigen: problems and perspectives. *Clin Nephrol* **66**:153–159.

Jenne DE, Tschopp J, Lüdemann J, Utecht B, and Gross WL (1990) Wegener's autoantigen decoded. *Nature* **346**:520.

Jennette JC, Falk RJ, and Gasim AH (2011) Pathogenesis of antineutrophil cytoplasmic autoantibody vasculitis. *Curr Opin Nephrol Hypertens* **20**:263–270.

Jeppsson JO, Laurell CB, and Fagerhol M (1978) Properties of isolated human alpha1-antitrypsins of Pi types M, S and Z. *Eur J Biochem* **83**:143–153.

Jerke U, Hernandez DP, Beaudette P, Korkmaz B, Dittmar G, and Kettritz R (2015) Neutrophil serine proteases exert proteolytic activity on endothelial cells. *Kidney Int* **88**:764–775.

Kam CM, Kerrigan JE, Dolman KM, Goldschmeding R, Von dem Borne AE, and Powers JC (1992a) Substrate and inhibitor studies on proteinase 3. *FEBS Lett* **297**:119–123.

Kam CM, Oglesby TJ, Pangburn MK, Volanakis JE, and Powers JC (1992b) Substituted isocoumarins as inhibitors of complement serine proteases. *J Immunol* **149**:163–168.

Kantari C, Millet A, Gabillet J, Hajjar E, Broemstrup T, Pluta P, Reuter N, and Witko-Sarsat V (2011) Molecular analysis of the membrane insertion domain of proteinase 3, the Wegener's autoantigen, in RBL cells: implication for its pathogenic activity. *J Leukoc Biol* **90**:941–950.

Kao RC, Wehner NG, Skubitz KM, Gray BH, and Hoidal JR (1988) Proteinase 3. A distinct human polymorphonuclear leukocyte proteinase that produces emphysema in hamsters. *J Clin Invest* **82**:1963–1973.

Kasperkiewicz P, Poreba M, Snipas SJ, Parker H, Winterbourn CC, Salvesen GS, and Drag M (2014) Design of ultrasensitive probes for human neutrophil elastase through hybrid combinatorial substrate library profiling. *Proc Natl Acad Sci USA* **111**:2518–2523.

Kawabata K, Suzuki M, Sugitani M, Imaki K, Toda M, and Miyamoto T (1991) ONO-5046, a novel inhibitor of human neutrophil elastase. *Biochem Biophys Res Commun* **177**:814–820.

Kessenbrock K, Dau T, and Jenne DE (2011) Tailor-made inflammation: how neutrophil serine proteases modulate the inflammatory response. *J Mol Med (Berl)* **89**:23–28.

Kettritz R (2008) Autoimmunity in kidney diseases. *Scand J Clin Lab Invest Suppl* **241**:99–103.

Kettritz R (2012) How anti-neutrophil cytoplasmic autoantibodies activate neutrophils. *Clin Exp Immunol* **169**:220–228.

Kiehntopf M, Schmerler D, Brunkhorst FM, Winkler R, Ludewig K, Osterloh D, Bloos F, Reinhart K, and Deufel T (2011) Mass spectrometry-based protein patterns in the diagnosis of sepsis/systemic inflammatory response syndrome. *Shock* **36**:560–569.

King AE, Critchley HO, Sallenave JM, and Kelly RW (2003) Elafin in human endometrium: an antiprotease and antimicrobial molecule expressed during menstruation. *J Clin Endocrinol Metab* **88**:4426–4431.

Knight WB, Maycock AL, Green BG, Ashe BM, Gale P, Weston H, Finke PE, Hagmann WK, Shah SK, and Doherty JB (1992) Mechanism of inhibition of human leukocyte elastase by two cephalosporin derivatives. *Biochemistry* **31**:4980–4986.

Koizumi M, Fujino A, Fukushima K, Kamimura T, and Takimoto-Kamimura M (2008) Complex of human neutrophil elastase with 1/2SLPI. *J Synchrotron Radiat* **15**:308–311.

Korkmaz B, Attucci S, Hazouard E, Ferrandiere M, Jourdan ML, Brillard-Bourdet M, Juliano L, and Gauthier F (2002) Discriminating between the activities of human neutrophil elastase and proteinase 3 using serpin-derived fluorogenic substrates. *J Biol Chem* **277**:39074–39081.

Korkmaz B, Attucci S, Jourdan ML, Juliano L, and Gauthier F (2005a) Inhibition of neutrophil elastase by alpha1-protease inhibitor at the surface of human polymorphonuclear neutrophils. *J Immunol* **175**:3329–3338.

Korkmaz B, Attucci S, Moreau T, Godat E, Juliano L, and Gauthier F (2004) Design and use of highly specific substrates of neutrophil elastase and proteinase 3. *Am J Respir Cell Mol Biol* **30**:801–807.

Korkmaz B, Hajjar E, Kalupov T, Reuter N, Brillard-Bourdet M, Moreau T, Juliano L, and Gauthier F (2007) Influence of charge distribution at the active site surface on the substrate specificity of human neutrophil protease 3 and elastase. A kinetic and molecular modeling analysis. *J Biol Chem* **282**:1989–1997.

Korkmaz B, Horwitz MS, Jenne DE, and Gauthier F (2010) Neutrophil elastase, proteinase 3, and cathepsin G as therapeutic targets in human diseases. *Pharmacol Rev* **62**:726–759.

Korkmaz B, Jaillet J, Jourdan ML, Gauthier A, Gauthier F, and Attucci S (2009) Catalytic activity and inhibition of Wegener antigen proteinase 3 on the cell surface of human polymorphonuclear neutrophils. *J Biol Chem* **284**:19896–19902.

Korkmaz B, Kellenberger C, Viaud-Massuard MC, and Gauthier F (2013a) Selective inhibitors of human neutrophil proteinase 3. *Curr Pharm Des* **19**:966–976.

Korkmaz B, Kuhl A, Bayat B, Santoso S, and Jenne DE (2008a) A hydrophobic patch on proteinase 3, the target of autoantibodies in Wegener granulomatosis, mediates membrane binding via NB1 receptors. *J Biol Chem* **283**:35976–35982.

Korkmaz B, Lesner A, Letast S, Mahdi YK, Jourdan ML, Dallet-Choisy S, Marchand-Adam S, Kellenberger C, Viaud-Massuard MC, and Jenne DE, et al. (2013b) Neutrophil proteinase 3 and dipeptidyl peptidase I (cathepsin C) as pharmacological targets in granulomatosis with polyangiitis (Wegener granulomatosis). *Semin Immunopathol* **35**:411–421.

Korkmaz B, Moreau T, and Gauthier F (2008b) Neutrophil elastase, proteinase 3 and cathepsin G: physicochemical properties, activity and physiopathological functions. *Biochimie* **90**:227–242.

Korkmaz B, Poutrain P, Hazouard E, de Monte M, Attucci S, and Gauthier FL (2005b) Competition between elastase and related proteases from human neutrophil for binding to alpha1-protease inhibitor. *Am J Respir Cell Mol Biol* **32**:553–559.

Krowarsch D, Cierpicki T, Jelen F, and Otlewski J (2003) Canonical protein inhibitors of serine proteases. *Cell Mol Life Sci* **60**:2427–2444.

Kuhl A, Korkmaz B, Utecht B, Kniepert A, Schönermarck U, Specks U, and Jenne DE (2010) Mapping of conformational epitopes on human proteinase 3, the auto-antigen of Wegener's granulomatosis. *J Immunol* **185**:387–399.

Laskowski M Jr and Kato I (1980) Protein inhibitors of proteinases. *Annu Rev Biochem* **49**:593–626.

Lechtenberg BC, Kasperkiewicz P, Robinson H, Drag M, and Riedl SJ (2015) The elastase-PK101 structure: mechanism of an ultrasensitive activity-based probe revealed. *ACS Chem Biol* **10**:945–951.

Lin SJ, Dong KC, Eigenbrot C, van Lookeren Campagne M, and Kirchhofer D (2014) Structures of neutrophil serine protease 4 reveal an unusual mechanism of substrate recognition by a trypsin-fold protease. *Structure* **22**:1333–1340.

Liu T, Fu G, Luo X, Liu Y, Wang Y, Wang RE, Schultz PG, and Wang F (2015) Rational design of antibody protease inhibitors. *J Am Chem Soc* **137**:4042–4045.

Loison F, Zhu H, Karatepe K, Kasorn A, Liu P, Ye K, Zhou J, Cao S, Gong H, and Jenne DE, et al. (2014) Proteinase 3-dependent caspase-3 cleavage modulates neutrophil death and inflammation. *J Clin Invest* **124**:4445–4458.

Lucas SD, Costa E, Guedes RC, and Moreira R (2013) Targeting COPD: advances on low-molecular-weight inhibitors of human neutrophil elastase. *Med Res Rev* **33** (Suppl 1):E73–E101.

Lyons PA, Rayner TF, Trivedi S, Holle JU, Watts RA, Jayne DR, Baslund B, Brenchley P, Bruchfeld A, and Chaudhry AN, et al. (2012) Genetically distinct subsets within ANCA-associated vasculitis. *N Engl J Med* **367**:214–223.

Mahr AD, Edberg JC, Stone JH, Hoffman GS, St Clair EW, Specks U, Dellaripa PF, Seo P, Spiera RF, and Rouhani FN, et al. (2010) Alpha₁-antitrypsin deficiency-related alleles Z and S and the risk of Wegener's granulomatosis. *Arthritis Rheum* **62**:3760–3767.

Mallen-St Clair J, Shi GP, Sutherland RE, Chapman HA, Caughey GH, and Wolters PJ (2006) Cathepsins L and S are not required for activation of dipeptidyl peptidase I (cathepsin C) in mice. *Biol Chem* **387**:1143–1146.

Mangan MS, Kaiserman D, and Bird PI (2008) The role of serpins in vertebrate immunity. *Tissue Antigens* **72**:1–10.

Marrero A, Duquerroy S, Trapani S, Goulas T, Guevara T, Andersen GR, Navaza J, Sottrup-Jensen L, and Gomis-Rüth FX (2012) The crystal structure of human α2-macroglobulin reveals a unique molecular cage. *Angew Chem Int Ed Engl* **51**:3340–3344.

Matheson NR, Gibson HL, Hallewell RA, Barr PJ, and Travis J (1986) Recombinant DNA-derived forms of human alpha 1-proteinase inhibitor. Studies on the alanine 358 and cysteine 358 substituted mutants. *J Biol Chem* **261**:10404–10409.

McBride JD, Freeman HN, and Leatherbarrow RJ (1999) Selection of human elastase inhibitors from a conformationally constrained combinatorial peptide library. *Eur J Biochem* **266**:403–412.

McGuire MJ, Lipsky PE, and Thiele DL (1993) Generation of active myeloid and lymphoid granule serine proteases requires processing by the granule thiol protease dipeptidyl peptidase I. *J Biol Chem* **268**:2458–2467.

Méthot N, Guay D, Rubin J, Ethier D, Ortega K, Wong S, Normandin D, Beaulieu C, Reddy TJ, and Riendeau D, et al. (2008) In vivo inhibition of serine protease processing requires a high fractional inhibition of cathepsin C. *Mol Pharmacol* **73**:1857–1865.

Méthot N, Rubin J, Guay D, Beaulieu C, Ethier D, Reddy TJ, Riendeau D, and Percival MD (2007) Inhibition of the activation of multiple serine proteases with a cathepsin C inhibitor requires sustained exposure to prevent pro-enzyme processing. *J Biol Chem* **282**:20836–20846.

Millet A, Martin KR, Bonnefoy F, Saas P, Mocek J, Alkan M, Terrier B, Kerstein A, Tamassia N, and Satyanarayanan SK, et al. (2015) Proteinase 3 on apoptotic cells disrupts immune silencing in autoimmune vasculitis. *J Clin Invest* **125**:4107–4121.

Monczak Y, Trudel M, Lamph WW, and Miller WH Jr (1997) Induction of apoptosis without differentiation by retinoic acid in PLB-985 cells requires the activation of both RAR and RXR. *Blood* **90**:3345–3355.

Nara K, Ito S, Ito T, Suzuki Y, Ghoneim MA, Tachibana S, and Hirose S (1994) Elastase inhibitor elafin is a new type of proteinase inhibitor which has a

transglutaminase-mediated anchoring sequence termed "cementoin". *J Biochem* **115**:441–448.

Nauseef WM and Borregaard N (2014) Neutrophils at work. *Nat Immunol* **15**: 602–611.

Navia MA, McKeever BM, Springer JP, Lin TY, Williams HR, Fluder EM, Dorn CP, and Hoogsteen K (1989) Structure of human neutrophil elastase in complex with a peptide chloromethyl ketone inhibitor at 1.84-A resolution. *Proc Natl Acad Sci USA* **86**:7–11.

Nobar SM, Zani ML, Boudier C, Moreau T, and Bieth JG (2005) Oxidized elafin and trappin poorly inhibit the elastolytic activity of neutrophil elastase and proteinase 3. *FEBS J* **272**:5883–5893.

Ohlsson K and Tegner H (1976) Inhibition of elastase from granulocytes by the low molecular weight bronchial protease inhibitor. *Scand J Clin Lab Invest* **36**: 437–445.

Olson ST and Gettins PG (2011) Regulation of proteases by protein inhibitors of the serpin superfamily. *Prog Mol Biol Transl Sci* **99**:185–240.

Owen CA and Campbell EJ (1999) The cell biology of leukocyte-mediated proteolysis. *J Leukoc Biol* **65**:137–150.

Owen MC, Brennan SO, Lewis JH, and Carrell RW (1983) Mutation of antitrypsin to antithrombin. alpha 1-antitrypsin Pittsburgh (358 Met leads to Arg), a fatal bleeding disorder. *N Engl J Med* **309**:694–698.

Pederzoli M, Kantari C, Gausson V, Moriceau S, and Witko-Sarsat V (2005) Proteinase-3 induces procaspase-3 activation in the absence of apoptosis: potential role of this compartmentalized activation of membrane-associated procaspase-3 in neutrophils. *J Immunol* **174**:6381–6390.

Pendergraft WF 3rd, Rudolph EH, Falk RJ, Jahn JE, Grimmler M, Hengst L, Jennette JC, and Preston GA (2004) Proteinase 3 sidesteps caspases and cleaves p21(Waf1/Cip1/Sdi1) to induce endothelial cell apoptosis. *Kidney Int* **65**:75–84.

Petersen CM (1993) Alpha 2-macroglobulin and pregnancy zone protein. Serum levels, alpha 2-macroglobulin receptors, cellular synthesis and aspects of function in relation to immunology. *Dan Med Bull* **40**:409–446.

Pfister H, Ollert M, Fröhlich LF, Quintanilla-Martinez L, Colby TV, Specks U, and Jenne DE (2004) Antineutrophil cytoplasmic autoantibodies against the murine homolog of proteinase 3 (Wegener autoantigen) are pathogenic in vivo. *Blood* **104**:1411–1418.

Pham CT (2006) Neutrophil serine proteases: specific regulators of inflammation. *Nat Rev Immunol* **6**:541–550.

Pham CT (2008) Neutrophil serine proteases fine-tune the inflammatory response. *Int J Biochem Cell Biol* **40**:1317–1333.

Pham CT, Ivanovich JL, Raptis SZ, Zehnbauer B, and Ley TJ (2004) Papillon-Lefèvre syndrome: correlating the molecular, cellular, and clinical consequences of cathepsin C/dipeptidyl peptidase I deficiency in humans. *J Immunol* **173**:7277–7281.

Popow-Stellmaszyk J, Wysocka M, Lesner A, Korkmaz B, and Rolka K (2013) A new proteinase 3 substrate with improved selectivity over human neutrophil elastase. *Anal Biochem* **442**:75–82.

Powers JC, Boone R, Carroll DL, Gupton BF, Kam CM, Nishino N, Sakamoto M, and Tuhy PM (1984) Reaction of azapeptides with human leukocyte elastase and porcine pancreatic elastase. New inhibitors and active site titrants. *J Biol Chem* **259**:4288–4294.

Pozzi N, Vogt AD, Gohara DW, and Di Cera E (2012) Conformational selection in trypsin-like proteases. *Curr Opin Struct Biol* **22**:421–431.

Preston GA, Zarella CS, Pendergraft WF 3rd, Rudolph EH, Yang JJ, Sekura SB, Jennette JC, and Falk RJ (2002) Novel effects of neutrophil-derived proteinase 3 and elastase on the vascular endothelium involve in vivo cleavage of NF-kappaB and proapoptotic changes in JNK, ERK, and p38 MAPK signaling pathways. *J Am Soc Nephrol* **13**:2840–2849.

Proulx C, Sabatino D, Hopewell R, Spiegel J, García Ramos Y, and Lubell WD (2011) Azapeptides and their therapeutic potential. *Future Med Chem* **3**:1139–1164.

Rao NV, Marshall BC, Gray BH, and Hoidal JR (1993) Interaction of secretory leukocyte protease inhibitor with proteinase-3. *Am J Respir Cell and Mol Biol* **8**:612–616.

Rao NV, Wehner NG, Marshall BC, Gray WR, Gray BH, and Hoidal JR (1991) Characterization of proteinase-3 (PR-3), a neutrophil serine proteinase. Structural and functional properties. *J Biol Chem* **266**:9540–9548.

Rees DD, Brain JD, Wohl ME, Humes JL, and Mumford RA (1997) Inhibition of neutrophil elastase in CF sputum by L-658,758. *J Pharmacol Exp Ther* **283**:1201–1206.

Remold-O'Donnell E, Nixon JC, and Rose RM (1989) Elastase inhibitor. Characterization of the human elastase inhibitor molecule associated with monocytes, macrophages, and neutrophils. *J Exp Med* **169**:1071–1086.

Rooney CP, Taggart C, Coakley R, McElvaney NG, and O'Neill SJ (2001) Anti-proteinase 3 antibody activation of neutrophils can be inhibited by alpha1-antitrypsin. *Am J Respir Cell Mol Biol* **24**:747–754.

Salahuddin P (2010) Genetic variants of alpha1-antitrypsin. *Curr Protein Pept Sci* **11**: 101–117.

Sallenave JM (2010) Secretory leukocyte protease inhibitor and elafin/trappin-2: versatile mucosal antimicrobials and regulators of immunity. *Am J Respir Cell Mol Biol* **42**:635–643.

Sallenave JM, Marsden MD, and Ryle AP (1992) Isolation of elafin and elastase-specific inhibitor (ESI) from bronchial secretions. Evidence of sequence homology and immunological cross-reactivity. *Biol Chem Hoppe Seyler* **373**:27–33.

Sallenave JM and Ryle AP (1991) Purification and characterization of elastase-specific inhibitor. Sequence homology with mucus proteinase inhibitor. *Biol Chem Hoppe Seyler* **372**:13–21.

Schalkwijk J, Chang A, Janssen P, De Jongh GJ, and Mier PD (1990) Skin-derived antileucoproteases (SKALPs): characterization of two new elastase inhibitors from psoriatic epidermis. *Br J Dermatol* **122**:631–641.

Schapira M, Ramus MA, Jallat S, Carvallo D, and Courtney M (1986) Recombinant alpha 1-antitrypsin Pittsburgh (Met 358——Arg) is a potent inhibitor of plasma kallikrein and activated factor XII fragment. *J Clin Invest* **77**:635–637.

Schechter I and Berger A (1967) On the size of the active site in proteases. I. Papain. *Biochem Biophys Res Commun* **27**:157–162.

Schreiber A, Busjahn A, Luft FC, and Kettritz R (2003) Membrane expression of proteinase 3 is genetically determined. *J Am Soc Nephrol* **14**:68–75.

Scott A, Weldon S, and Taggart CC (2011) SLPI and elafin: multifunctional antiproteases of the WFDC family. *Biochem Soc Trans* **39**:1437–1440.

Scott CF, Carrell RW, Glaser CB, Kueppers F, Lewis JH, and Colman RW (1986) Alpha-1-antitrypsin-Pittsburgh. A potent inhibitor of human plasma factor XIa, kallikrein, and factor XIIf. *J Clin Invest* **77**:631–634.

Selga D, Segelmark M, Wieslander J, Gunnarsson L, and Hellmark T (2004) Epitope mapping of anti-PR3 antibodies using chimeric human/mouse PR3 recombinant proteins. *Clin Exp Immunol* **135**:164–172.

Sieńczyk M and Oleksyszyn J (2009) Irreversible inhibition of serine proteases - design and in vivo activity of diaryl alpha-aminophosphonate derivatives. *Curr Med Chem* **16**:1673–1687.

Silva F, Hummel AM, Jenne DE, and Specks U (2010) Discrimination and variable impact of ANCA binding to different surface epitopes on proteinase 3, the Wegener's autoantigen. *J Autoimmun* **35**:299–308.

Silverman GA, Bird PI, Carrell RW, Church FC, Coughlin PB, Gettins PG, Irving JA, Lomas DA, Luke CJ, and Moyer RW, et al. (2001) The serpins are an expanding superfamily of structurally similar but functionally diverse proteins. Evolution, mechanism of inhibition, novel functions, and a revised nomenclature. *J Biol Chem* **276**:33293–33296.

Sinden NJ, Baker MJ, Smith DJ, Kreft JU, Dafforn TR, and Stockley RA (2015) α-1-antitrypsin variants and the proteinase/antiproteinase imbalance in chronic obstructive pulmonary disease. *Am J Physiol Lung Cell Mol Physiol* **308**: L179–L190.

Sinden NJ and Stockley RA (2013) Proteinase 3 activity in sputum from subjects with alpha-1-antitrypsin deficiency and COPD. *Eur Respir J* **41**:1042–1050.

Sørensen OE, Clemmensen SN, Dahl SL, Østergaard O, Heegaard NH, Glenthøj A, Nielsen FC, and Borregaard N (2014) Papillon-Lefèvre syndrome patient reveals species-dependent requirements for neutrophil defenses. *J Clin Invest* **124**: 4539–4548.

Sottrup-Jensen L (1989) Alpha-macroglobulins: structure, shape, and mechanism of proteinase complex formation. *J Biol Chem* **264**:11539–11542.

Specks U (2000) What you should know about PR3-ANCA. Conformational requirements of proteinase 3 (PR3) for enzymatic activity and recognition by PR3-ANCA. *Arthritis Res* **2**:263–267.

Specks U, Fass DN, Fautsch MP, Hummel AM, and Viss MA (1996) Recombinant human proteinase 3, the Wegener's autoantigen, expressed in HMC-1 cells is enzymatically active and recognized by c-ANCA. *FEBS Lett* **390**:265–270.

Specks U, Wiegert EM, and Homburger HA (1997) Human mast cells expressing recombinant proteinase 3 (PR3) as substrate for clinical testing for anti-neutrophil cytoplasmic antibodies (ANCA). *Clin Exp Immunol* **109**:286–295.

Stawikowski M, Stawikowska R, Jaśkiewicz A, Zabłotna E, and Rolka K (2005) Examples of peptide-peptoid hybrid serine protease inhibitors based on the trypsin inhibitor SFTI-1 with complete protease resistance at the P1-P1′ reactive site. *ChemBioChem* **6**:1057–1061.

Stolley JM, Gong D, Farley K, Zhao P, Cooley J, Crouch EC, Benarafa C, and Remold-O'Donnell E (2012) Increased surfactant protein D fails to improve bacterial clearance and inflammation in serpinB1-/- mice. *Am J Respir Cell Mol Biol* **47**: 792–799.

Sturrock AB, Espinosa R 3rd, Hoidal JR, and Le Beau MM (1993) Localization of the gene encoding proteinase-3 (the Wegener's granulomatosis autoantigen) to human chromosome band 19p13.3. *Cytogenet Cell Genet* **64**:33–34.

Sturrock A, Franklin KF, and Hoidal JR (1996) Human proteinase-3 expression is regulated by PU.1 in conjunction with a cytidine-rich element. *J Biol Chem* **271**: 32392–32402.

Sturrock AB, Franklin KF, Rao G, Marshall BC, Rebentisch MB, Lemons RS, and Hoidal JR (1992) Structure, chromosomal assignment, and expression of the gene for proteinase-3. The Wegener's granulomatosis autoantigen. *J Biol Chem* **267**:21193–21199.

Sun J, Fass DN, Viss MA, Hummel AM, Tang H, Homburger HA, and Specks U (1998) A proportion of proteinase 3 (PR3)-specific anti-neutrophil cytoplasmic antibodies (ANCA) only react with PR3 after cleavage of its N-terminal activation dipeptide. *Clin Exp Immunol* **114**:320–326.

Sundberg EJ and Mariuzza RA (2002) Molecular recognition in antibody-antigen complexes. *Adv Protein Chem* **61**:119–160.

Tadema H, Heeringa P, and Kallenberg CG (2011) Bacterial infections in Wegener's granulomatosis: mechanisms potentially involved in autoimmune pathogenesis. *Curr Opin Rheumatol* **23**:366–371.

Teshima T, Griffin JC, and Powers JC (1982) A new class of heterocyclic serine protease inhibitors. Inhibition of human leukocyte elastase, porcine pancreatic elastase, cathepsin G, and bovine chymotrypsin A with substituted benzoxazinones, quinazolines, and anthranilates. *J Biol Chem* **257**:5085–5091.

Thun GA, Imboden M, Ferrarotti I, Kumar A, Obeidat M, Zorzetto M, Haun M, Curjuric I, Alves AC, and Jackson VE, et al. (2013) Causal and synthetic associations of variants in the SERPINA gene cluster with alpha1-antitrypsin serum levels. *PLoS Genet* **9**: DOI:10.1371/journal.pgen.1003585.

Travis J, Owen M, George P, Carrell R, Rosenberg S, Hallewell RA, and Barr PJ (1985) Isolation and properties of recombinant DNA produced variants of human alpha 1-proteinase inhibitor. *J Biol Chem* **260**:4384–4389.

Travis J and Salvesen GS (1983) Human plasma proteinase inhibitors. *Annu Rev Biochem* **52**:655–709.

Tremblay GM, Sallenave JM, Israél-Assayag E, Cormier Y, and Gauldie J (1996) Elafin/elastase-specific inhibitor in bronchoalveolar lavage of normal subjects and farmer's lung. *Am J Respir Crit Care Med* **154**:1092–1098.

Tsunemi M, Matsuura Y, Sakakibara S, and Katsube Y (1996) Crystal structure of an elastase-specific inhibitor elafin complexed with porcine pancreatic elastase determined at 1.9 A resolution. *Biochemistry* **35**:11570–11576.

Turk D, Janjić V, Stern I, Podobnik M, Lamba D, Dahl SW, Lauritzen C, Pedersen J, Turk V, and Turk B (2001) Structure of human dipeptidyl peptidase I (cathepsin

C): exclusion domain added to an endopeptidase framework creates the machine for activation of granular serine proteases. *EMBO J* **20**:6570–6582.

Van der Geld YM, Limburg PC, and Kallenberg CG (1999) Characterization of monoclonal antibodies to proteinase 3 (PR3) as candidate tools for epitope mapping of human anti-PR3 autoantibodies. *Clin Exp Immunol* **118**:487–496.

van der Geld YM, Oost-Kort W, Limburg PC, Specks U, and Kallenberg CG (2000) Recombinant proteinase 3 produced in different expression systems: recognition by anti-PR3 antibodies. *J Immunol Methods* **244**:117–131.

van der Geld YM, Tool AT, Videler J, de Haas M, Tervaert JW, Stegeman CA, Limburg PC, Kallenberg CG, and Roos D (2002) Interference of PR3-ANCA with the enzymatic activity of PR3: differences in patients during active disease or remission of Wegener's granulomatosis. *Clin Exp Immunol* **129**:562–570.

Vega-Carrascal I, Reeves EP, Niki T, Arikawa T, McNally P, O'Neill SJ, Hirashima M, and McElvaney NG (2011) Dysregulation of TIM-3-galectin-9 pathway in the cystic fibrosis airways. *J Immunol* **186**:2897–2909.

Vigl K, Monshi B, Vujic I, and Rappersberger K (2015) Pyoderma gangrenosum-like necrotizing panniculitis associated with alpha-1 antitrypsin deficiency: a lethal course. *J Dtsch Dermatol Ges* **13**:1180–1184.

Virca GD and Travis J (1984) Kinetics of association of human proteinases with human alpha 2-macroglobulin. *J Biol Chem* **259**:8870–8874.

Vogelmeier C, Biedermann T, Maier K, Mazur G, Behr J, Krombach F, and Buhl R (1997) Comparative loss of activity of recombinant secretory leukoprotease inhibitor and alpha 1-protease inhibitor caused by different forms of oxidative stress. *Eur Respir J* **10**:2114–2119.

von Vietinghoff S, Tunnemann G, Eulenberg C, Wellner M, Cristina Cardoso M, Luft FC, and Kettritz R (2007) NB1 mediates surface expression of the ANCA antigen proteinase 3 on human neutrophils. *Blood* **109**:4487–4493.

Vos JB, van Sterkenburg MA, Rabe KF, Schalkwijk J, Hiemstra PS, and Datson NA (2005) Transcriptional response of bronchial epithelial cells to Pseudomonas aeruginosa: identification of early mediators of host defense. *Physiol Genomics* **21**:324–336.

Wang L, Li Q, Wu L, Liu S, Zhang Y, Yang X, Zhu P, Zhang H, Zhang K, and Lou J, et al. (2013) Identification of SERPINB1 as a physiological inhibitor of human granzyme H. *J Immunol* **190**:1319–1330.

Wei AZ, Mayr I, and Bode W (1988) The refined 2.3 A crystal structure of human leukocyte elastase in a complex with a valine chloromethyl ketone inhibitor. *FEBS Lett* **234**:367–373.

Wesolowski J, Alzogaray V, Reyelt J, Unger M, Juarez K, Urrutia M, Cauerhff A, Danquah W, Rissiek B, and Scheuplein F, et al. (2009) Single domain antibodies: promising experimental and therapeutic tools in infection and immunity. *Med Microbiol Immunol (Berl)* **198**:157–174.

Wiedow O, Lüademann J, and Utecht B (1991) Elafin is a potent inhibitor of proteinase 3. *Biochem Biophys Res Commun* **174**:6–10.

Wiedow O, Schröder JM, Gregory H, Young JA, and Christophers E (1990) Elafin: an elastase-specific inhibitor of human skin. Purification, characterization, and complete amino acid sequence. *J Biol Chem* **265**:14791–14795.

Wilkinson RD, Williams R, Scott CJ, and Burden RE (2015) Cathepsin S: therapeutic, diagnostic, and prognostic potential. *Biol Chem* **396**:867–882.

Wilkinson TS, Roghanian A, Simpson AJ, and Sallenave JM (2011) WAP domain proteins as modulators of mucosal immunity. *Biochem Soc Trans* **39**:1409–1415.

Witko-Sarsat V, Cramer EM, Hieblot C, Guichard J, Nusbaum P, Lopez S, Lesavre P, and Halbwachs-Mecarelli L (1999) Presence of proteinase 3 in secretory vesicles: evidence of a novel, highly mobilizable intracellular pool distinct from azurophil granules. *Blood* **94**:2487–2496.

Witko-Sarsat V, Halbwachs-Mecarelli L, Almeida RP, Nusbaum P, Melchior M, Jamaleddine G, Lesavre P, Descamps-Latscha B, and Gabay JE (1996) Characterization of a recombinant proteinase 3, the autoantigen in Wegener's granulomatosis and its reactivity with anti-neutrophil cytoplasmic autoantibodies. *FEBS Lett* **382**:130–136.

Wong ET, Jenne DE, Zimmer M, Porter SD, and Gilks CB (1999) Changes in chromatin organization at the neutrophil elastase locus associated with myeloid cell differentiation. *Blood* **94**:3730–3736.

Wysocka M, Lesner A, Gruba N, Korkmaz B, Gauthier F, Kitamatsu M, Łęgowska A, and Rolka K (2012) Three wavelength substrate system of neutrophil serine proteinases. *Anal Chem* **84**:7241–7248.

Ying QL and Simon SR (2001) Kinetics of the inhibition of proteinase 3 by elafin. *Am J Respir Cell Mol Biol* **24**:83–89.

Zani ML, Baranger K, Guyot N, Dallet-Choisy S, and Moreau T (2009) Protease inhibitors derived from elafin and SLPI and engineered to have enhanced specificity towards neutrophil serine proteases. *Protein Sci* **18**:579–594.

Zani ML, Nobar SM, Lacour SA, Lemoine S, Boudier C, Bieth JG, and Moreau T (2004) Kinetics of the inhibition of neutrophil proteinases by recombinant elafin and pre-elafin (trappin-2) expressed in Pichia pastoris. *Eur J Biochem* **271**:2370–2378.

Zega A (2005) Azapeptides as pharmacological agents. *Curr Med Chem* **12**:589–597.

Zeng W, Silverman GA, and Remold-O'Donnell E (1998) Structure and sequence of human M/NEI (monocyte/neutrophil elastase inhibitor), an Ov-serpin family gene. *Gene* **213**:179–187.

Zhang R, Durkin JP, and Windsor WT (2002) Azapeptides as inhibitors of the hepatitis C virus NS3 serine protease. *Bioorg Med Chem Lett* **12**:1005–1008.

Zhong J and Groutas WC (2004) Recent developments in the design of mechanism-based and alternate substrate inhibitors of serine proteases. *Curr Top Med Chem* **4**:1203–1216.

Zimmer M, Medcalf RL, Fink TM, Mattmann C, Lichter P, and Jenne DE (1992) Three human elastase-like genes coordinately expressed in the myelomonocyte lineage are organized as a single genetic locus on 19pter. *Proc Natl Acad Sci USA* **89**:8215–8219.

Zoega M, Ravnsborg T, Højrup P, Houen G, and Schou C (2012) Proteinase 3 carries small unusual carbohydrates and associates with αlpha-defensins. *J Proteomics* **75**:1472–1485.

Zuckermann RN (2011) Peptoid origins. *Biopolymers* **96**:545–555.